Chemical Reviews

Volume 90, Number 2 March/April 1990

The Photophysics of Chromium(III) Complexes

LESLIE S. FORSTER

Department of Chemistry, University of Arizona, Tucson, Arizona 85721

Received April 11, 1989 (Revised Manuscript Received November 6, 1989)

Contents

Leslie S. Forster was born in Chicago in 1924 and grew up in Los Angeles. He attended UCLA and received the B.S. degree from the University of California, Berkeley, in 1947. He received the Ph.D. degree in 1951 from the University of Minnesota under the direction of Robert Livingston and was a Postdoctoral Fellow with W. A. Noyes, Jr., in 1951–1952. After 3 years as an instructor at Bates College, he joined the faculty of the University of Arizona, where he is now Professor of Chemistry. His research has been concerned with relaxation of excited electronic states in metal complexes and biological materials.

I. Abbreviations

acac	2,4-pentanedione
atp	antipyrene
bpy	2,2′-bipyridine
chda	*trans*-1,2-diaminocyclohexane
cyc*a*	*meso*-5,5,7,12,12,14-hexamethyl-1,4,8,11-tetraazacyclotetradecane
cyc*b*	*rac*-5,5,7,12,12,14-hexamethyl-1,4,8,11-tetraazacyclotetradecane
cyclam	1,4,8,11-tetraazacyclotetradecane
diamsar	1,8-diamino-3,6,10,13,16,19-hexaazabicyclo[6.6.6]eicosane
dien	bis(2-aminoethyl)amine
ditn	bis(3-aminopropyl)amine
DMF	dimethylformamide
DMSO	dimethyl sulfoxide
dmtc	dimethyldithiocarbamate
dtc	diethyldithiocarbamate
dtne	1,2-bis(1,4,7-triaza-1-cyclononyl)ethane
en	1,2-diaminoethane
etam	ethylamine
exan	ethyl xanthate
ida	iminodiacetate
imid	imidazolidone
meam	methylamine
mida	(methylimino)diacetate
mxan	methyl xanthate
ox	oxalate
oxine	8-hydroxyquinoline
pdc	pyridine-2,6-dicarboxylate
phen	1,10-phenanthroline
pic	2-picolylamine
pn	1,2-diaminopropane
py	pyridine
sen	4,4′,4″-ethylidynetris(3-azabutan-1-amine)
sep	(*S*)-1,3,6,8,10,13,16,19-octaazabicyclo[6.6.6]eicosane
tacn	1,4,7-triazacyclononane
tcta	1,4,7-triazacyclononane-*N*,*N*′,*N*″-triacetate

0009-2665/90/0790-0331$09.50/0

teta	5,12-*meso*-5,7,7,12,14,14-hexamethyl-1,4,8,11-tetraazacyclotetradecane
tetb	5,12-*rac*-5,7,7,12,14,14-hexamethyl-1,4,8,11-tetraazacyclotetradecane
tgl	thioglycolate
tn	1,3-diaminopropane
tox	thiooxalate

II. Introduction

Cr(III) luminescence has been known for more than a century. In 1867 E. Becquerel not only described the emission spectra of several solids containing Cr(III) as impurity centers but determined the lifetime of ruby with a phosphoroscope.[1] The 13-ms value he obtained is remarkably close to the lifetime of highly doped Cr^{3+}:Al_2O_3.[2] In the period between the Becquerel work and 1940, when Van Vleck interpreted the spectrum of chrome alum in terms of crystal field theory,[3] a few studies of Cr(III) emission, primarily in ionic crystals, were published.

After the renaissance of crystal field theory and its extension to ligand field theory in 1951, many solution absorption spectra of transition-metal complexes were recorded. The first report of luminescence from a Cr(III) complex in 1961[4] was quickly followed by studies in several laboratories.[5-7] In the intervening period, interest in this area has contained unabated and the literature on Cr(III) emission is more extensive than for any other transition-metal ion.

The metal ion in a complex is coupled so strongly to the ligands that the species persists in the liquid and, in some cases, the gas phase. Coordination complexes of transition-metal ions are in every sense well-defined molecular species and are distinguished from impurity centers in ionic solids where the coordination is disrupted when the crystal or glass melts. The properties of impurity centers are sensitive to the lattice parameters and, although there are similarities in the luminescence behavior of Cr(III) in a complex and as an impurity center, the focus in this review is on the effect of molecular structure, environment, and temperature on the luminescence of complexes. Only limited reference will be made to ionic solids.

The luminescence yield and lifetime depend upon the radiative and nonradiative rates. Photophysics is concerned with all processes that originate in excited electronic states but do not result directly in a permanent chemical change. Photochemistry and photophysical processes are often interrelated, but need not be. Nonetheless, mechanistic photochemistry leans heavily on photophysical data.

The conceptual basis for the current theories of radiationless transitions was established in the sixties, but the initial applications of the theory were mainly to aromatic molecules (for reviews, see refs 8–10). The first application of the theory of radiationless transitions to Cr(III) emission in 1970[11] was quickly followed by the work of Robbins and Thomson.[12] These two papers laid the groundwork for the theoretical interpretation of nonradiative decay in metal complexes. From the point of view of radiationless transitions theory, d–d transitions are intermediate between the well-shielded f–f transitions in lanthanide complexes and π–π^* transitions in organic molecules where extensive delocalization obtains. In the lanthanide complexes there is hardly any difference in the ground- and excited-state geometries, while substantial geometry changes accompany π-electron excitation. The geometry changes are small to moderate in metal-centered d–d transitions.

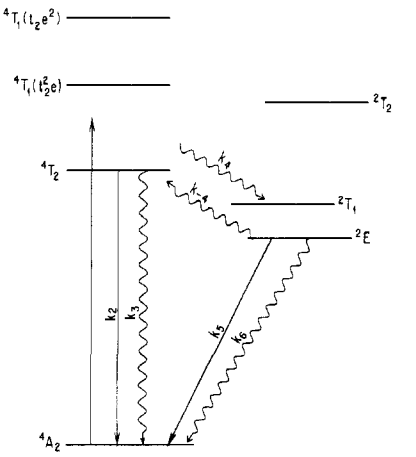

Figure 1. Energy levels and rate constants for Cr(III) complexes.

The large number of very stable Cr(III) complexes that have been prepared, coupled with the nearly universal emission from these complexes at low temperatures, has led to a very extensive literature detailing the photophysical properties of these systems. The work prior to 1969 has been reviewed.[13] Schläfer's last paper was devoted to the luminescence of Cr(III) complexes[14] and several other limited surveys have appeared in the interim[15-18] but no comprehensive treatment of this area has been made in the past two decades. In this review an effort has been made to collect all of the extant information and to attempt a systematic and critical treatment of the several facets of Cr(III) photophysics.

III. Spectra

In this section emphasis is on those aspects of the spectroscopy that are relevant to the interpretation of the Cr(III) photophysics.

A. Energy Levels

The terms representing the 120 states of the d^3 configuration are classified as quartet and doublet. The energy levels of d^3 ions in octahedral symmetry are displayed in Figure 1. The ground $^4A_2$ level and the three lowest doublet levels, ^2E, $^2T_1$, and $^2T_2$, are derived from the t_2^3 configuration. The lowest excited quartet states, $^4T_2$ and $^4T_1$, are derived from t_2^2e. The parity designations g and u are omitted here. The complete d^3 strong-field matrices have been published.[19] The diagonal elements of $^4A_2$, ^2E, and $^2T_1$ are independent of the octahedral field strength, Dq, while the $^4T_2$ and $^4T_1$ energies are proportional to Dq. The ^2E and $^2T_1$ diagonal elements are identical, but the degeneracy is removed through configuration interaction. Although the variation of the doublet-state energies with Dq is small, the ^2E energy does depend upon the interelectronic repulsion.[5]

The absorption spectra typically consist of two broad spin-allowed bands, $^4T_2 \leftarrow {}^4A_2$ and $^4T_1(t_2^2e) \leftarrow {}^4A_2$. Sometimes a third ligand field band, $^4T_1(t_2e^2) \leftarrow {}^4A_2$, is also observed, but this transition is often obscured by the more intense charge-transfer bands. ϵ_{max} for the

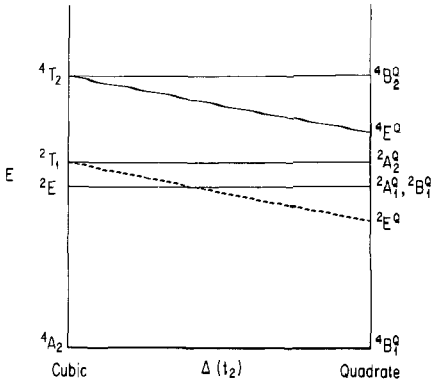

Figure 2. Level splittings (schmetic) in quadrate fields.

spin-allowed transitions are usually less than 100 M^{-1} cm^{-1}. The weaker narrow spin-forbidden lines ($\epsilon_{max} <$ 5) are due to the intraconfigurational (t_2^3) transitions, $^2T_2 \leftarrow {}^4A_2$, $^2T_1 \leftarrow {}^4A_2$, and $^2E \leftarrow {}^4A_2$. When the ligands have delocalized π-electron systems, relatively intense bands appear at low energies and obscure some of the metal-localized d–d absorption bands. These bands are associated with ligand-localized singlet–triplet transitions that are intensified by coupling with the unpaired Cr(III) d electrons, not by spin–orbit coupling.[20] In $Cr(acac)_3$ only the $^4T_2 \leftarrow {}^4A_2$ band is observed, and in $Cr(bpy)_3^{3+}$ even the lowest energy ligand field band is buried under a more intense intraligand transition.

The environment of Cr^{3+} is accurately O_h only in a few ionic crystals.[21-24] When Cr(III) is part of a CrX_6 molecule, the Cr^{3+} site symmetry can be close to O_h, but in most complexes the spectral assignments cannot be made in terms of strict O_h symmetry. For convenience, the complexes are classified as pseudooctahedral, trigonal, or quadrate, depending upon the approximate skeletal symmetry. As the symmetry deviates from octahedral the level degeneracies are progressively removed, but the twofold Kramers degeneracy remains. For notational simplicity, the pseudooctahedral symbols will be retained here, even when the actual symmetry is much lower, for those levels whose energies are not sensitive to the symmetry, e.g., ^2E and $^4A_2$. When the quadrate splittings are large in D_{4h}, C_{4h}, and C_{2v} complexes, the symmetry labels appropriate to tetragonal symmetry will be used. These are designated by the superscript Q (Figure 2).

In O_h symmetry, e.g., Cr^{3+}:MgO, ^2E is unsplit. ^2E is split in trigonal fields as exemplified by the 29-cm^{-1} value in ruby.[25] In crystals containing homoliganded complexes, the ^2E splittings range from 4–9 cm^{-1} for $Cr(NH_3)_6^{3+}$ in different lattices[26] to 20 cm^{-1} for $Cr(ox)_3^{3-}$[27] and 19 cm^{-1} in $Cr(en)_3^{3+}$.[28] The CD spectra of several homoliganded CrN_6 complexes indicate a reduction in the ^2E splittings from 70–150 cm^{-1} in a glass to 18 cm^{-1} in a single crystal.[29] Even in the strongly trigonally distorted $Cr(bpy)_3^{3+}$ the splitting is only 20 cm^{-1}.[30] A 56-cm^{-1} splitting in the emission spectrum of $Cr(acac)_3$ diluted into $Al(acac)_3$ was ascribed to the separation of the ^2E components.[31] However, the source of this spectral structure is multiple crystalline sites.[32-34] A very weak feature in absorption has been assigned to the upper ^2E component.[33] If this is correct, the ^2E splitting in Cr^3:$Al(acac)_3$ is 248 cm^{-1}, a remarkably large value.

^2E splittings approaching 300 cm^{-1} were suggested for some tetragonal complexes,[35,36] but these assignments have been questioned.[37,38] In the earlier work small splittings (<20 cm^{-1}) were not resolved. The low-temperature spectrum of $Cr(NH_3)_5NCO^{2+}$ was recorded at 1-cm^{-1} resolution in a crystalline medium and the smallest splitting in this complex, 218 cm^{-1}, was assigned to the ^2E components.[39] A 16-cm^{-1} separation was detected in the lowest excited doublet level of $[Cr(NH_3)_5Cl]Cl_2$, and this was identified as the ^2E splitting.[38] However, site-selective spectroscopy has demonstrated[40] that the ^2E splittings are indeed 175 cm^{-1} in $[Cr(NH_3)_5Cl]Cl_2$ and 206 cm^{-1} in $[Cr(NH_3)_5(H_2O)](ClO_4)_3$ as originally claimed.[35] An extensive examination of the $Cr(NH_3)_5X^{2+}$ (X = Cl^-, Br^-, I^-) absorption spectra in different lattices indicates that the small splittings are lattice dependent and due to multiple sites while the intramolecular ^2E splittings are in the 150–300-cm^{-1} range.[41]

It is now evident that low symmetry fields can split ^2E by more than 100 cm^{-1}. The question of the ^2E splitting magnitude is related to the adequacy of ligand field calculations for these small energy differences and to the analysis of the photophysical rates.

$^2T_1$ lies ≈600 cm^{-1} above ^2E in octahedral complexes.[42] The $^2T_1$ splitting is very sensitive to deviations from cubic symmetry. The effect of quadrate fields is shown in Figure 2. When the quadrate field is very large as in *trans*-$Cr(py)_4F_2^+$, the lower $^2T_1$ component, $^2E^Q$, lies below ^2E.[43] $^4T_2$ and $^4T_1$ are also split by noncubic fields. Two semiempirical approaches have been developed to compute the energy levels in quadrate complexes. In the first, the energy matrices are formulated in terms of two global crystal field parameters, *Ds* and *Dt*, which depend upon the structure of the entire complex.[44,45] In the other treatment, the angular overlap model (AOM) in the so-called additive approximation, the matrix elements are functions of the σ and π parameters for the individual ligands.[46,47] *Ds* and *Dt* are related to the AOM parameters for quadrate complexes.[46,48] The quadrate field parameter, $\Delta(t_2)$, in Figure 2 corresponds to the energy difference within the t_2 orbital set. The $^2E^Q$ energy is depressed by configuration interaction, mainly with a component of $^2T_2$, while $^2A_2^Q$ is little affected by noncubic fields. To a first approximation the $^2T_1$ splitting in quadrate complexes is $[\Delta(t_2)]^2/(6B + 2C)$, where B and C are the Racah parameters. $\Delta(t_2)$ depends only on the difference between the π-donation propensities of the axial and equatorial ligands. On the other hand, the $^4T_2$ and $^4T_1$ splittings depend linearly on differences in both the σ- and π-donation parameters. Consequently, the splittings in $^2T_1$ and $^4T_2$ will not vary with molecular structure in a parallel fashion, and the band structure in the spin-allowed absorption spectrum cannot be used to infer the magnitude of the $^2T_1$ splitting. The $^2T_1$ and ^2E splittings are sensitive to angular distortions, but the AOM treatment has not been very successful for the estimation of these small energy differences.[49]

B. Emission Spectra

A very useful guide to the assignment of metal complex emission spectra is: emission originates in the lowest excited level or any levels in thermal equilibrium with it.[50] With the exception of the weak emissions in some fluid solutions that have been assigned as prompt $^4T_2 \rightarrow {}^4A_2$,[51] this principle is obeyed by Cr(III) com-

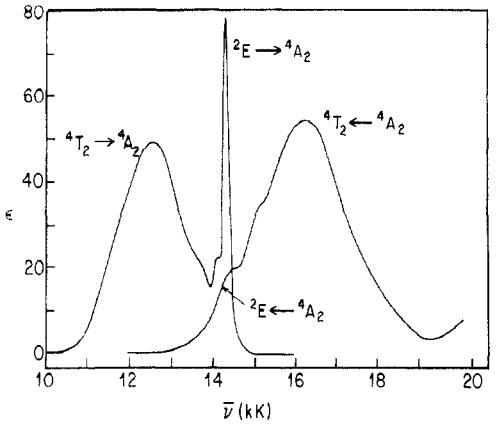

Figure 3. Absorption (298 K) and emission (78 K) spectra of $Cr(urea)_6^{3+}$ in methanol/ethylene glycol/H_2O (2:2:3 (v/v)). Redrawn from ref 7.

plexes. In pseudooctahedral and trigonal complexes the emission in the low-temperature limit will be either $^4T_2 \rightarrow {}^4A_2$ fluorescence or $^2E \rightarrow {}^4A_2$ phosphorescence, depending upon the magnitude of *Dq*. The early observation of dual emission from $Cr(urea)_6^{3+}$[7] (Figure 3) was a consequence of thermally induced fluorescence which disappears at sufficiently low temperatures.[52,53]

Schläfer suggested that $^4T_2$ and ^2E would be equienergetic in homoliganded complexes if the energy difference between the $^4T_2 \leftarrow {}^4A_2$ absorption band maximum and the $^2E \rightarrow {}^4A_2$ emission origin is approximately 2000 cm^{-1}.[54] Fleischauer et al. proposed that the $^4T_2$ energy could be estimated from the empirical equation $E(^4T_2) = 1.11\bar{\nu}_{0.05} - 0.88$, where $\bar{\nu}_{0.05}$ is in 10^3 cm^{-1} and denotes the position at which the $^4T_2 \leftarrow {}^4A_2$ absorption intensity has fallen to 5% of the maximum value.[55] This equation leads to roughly the same results as Schläfer's rule. For nitrogen coordination ^2E is invariably below $^4T_2$ and phosphorescence is the dominant emission in CrN_6 complexes. *Dq* is small enough with halogen coordination to make fluorescence the principal emission in $CrCl_6^{3-}$ and CrF_6^{3-} at 87 K.[14,54] However, the fluorescence from CrF_6^{3-} disappears at 4 K,[53] indicating that the ^2E and $^4T_2$ energies are nearly equal, with ^2E slightly lower.

The emission in CrO_6 complexes can be phosphorescence or fluorescence. Only phosphorescence is observed at all temperatures in $Cr(acac)_3$[31,56] and $Cr(ox)_3^{3-}$.[27,57] ^2E and $^4T_2$ are proximate in $Cr(urea)_6^{3+}$ and $Cr(atp)_6^{3+}$ as indicated by the thermally induced fluorescence.[52,58,59] Although ^2E is the lowest excited state in $Cr(H_2O)_6^{3+}$, it is only slightly below $^4T_2$.[60,61] According to Schläfer's rule and the positions of the $^4T_2 \leftarrow {}^4A_2$ and $^2E \rightarrow {}^4A_2$ bands in the spectra of CrO_6, where the oxygen coordination is via sulfinate ligands, the emission should be fluorescence in the sulfinato complexes.[62] The broad emission near 12000 cm^{-1} from these complexes at 90 K confirms this expectation.

Because the ^2E and $^4T_2$ levels are nearly coincident when Cr^{3+} is surrounded by six oxide ions, the character of the emission is very sensitive to the Cr–O distances in ionic crystals. $^4T_2$ in ruby is 2300 cm^{-1} above ^2E and only $^2E \rightarrow {}^4A_2$ occurs, while in emerald $^4T_2$ is 400 cm^{-1} below ^2E and fluorescence is the dominant emission.[63] Fluorescence is thermally induced in alexandrite, where $^4T_2$ is 800 cm^{-1} above ^2E.[64] In Cr^{3+}:MgO, charge compensation dictates at least two types of sites. The emission from Cr^{3+} in cubic sites is phosphorescence and that from noncubic sites is fluorescence.[65,66] When Cr^{3+} is dissolved in oxide glasses and glass ceramics, there is extensive site heterogeneity; both the sharp phosphorescence and the broad fluorescence often appear in the same system.[67,68] A similar sensitivity of the relative ^2E and $^4T_2$ dispositions to environment is found in $Cr(urea)_6^{3+}$, $Cr(atp)_6^{3+}$,[52] and $Cr(DMSO)_6^{3+}$.[69] The consequences of this site heterogeneity on the emission dynamics will be discussed in section IV.C.5.

Emission from several CrS_6 complexes has been described.[70] The emission is shifted to lower energies relative to CrN_6 complexes (Tables I and II). The narrow $Cr(exan)_3$ band at 12800 cm^{-1} is clearly $^2E \rightarrow {}^4A_2$. The emission from $Cr(dtc)_3$ is somewhat broader but still assignable as predominantly $^2E \rightarrow {}^4A_2$.[71] Other CrS_6 complexes exhibit much broader emission spectra which were assigned as $^4T_2 \rightarrow {}^4A_2$. However, in several cases, part of the broad emission was shown to arise from impurities, and the fluorescence assignments have been questioned.[71] Although the $Cr(dtox)_3^{3-}$ emission is fairly broad, the position of the $^4T_2 \leftarrow {}^4A_2$ absorption maximum[70] suggests that $^4T_2$ is above ^2E. The broad emission in $Cr(dmtc)_3$ has been attributed to extensive $^4T_2$–^2E mixing attendant upon the nearly equal energies of the two levels.[72] Vibronic mixing is not simply correlated with the energy difference between the $^4T_2$ and ^2E levels.[73] The available data indicate that the only homoliganded molecular complexes in which $^4T_2$ lies below ^2E are those with sulfinate coordination. In other systems where $^4T_2$ is the lowest excited state, Cr(III) is embedded in ionic crystals.

In O_h sites the 0–0 band of the $^2E_g \leftrightarrow {}^4A_{2g}$ transition is magnetic dipole allowed and very weak.[21] The bulk of the intensity is then concentrated in the vibronic sidebands. The nominally octahedral complexes $Cr(NCS)_6^{3-}$ and $Cr(CN)_6^{3-}$ are in slightly noncentrosymmetric sites in crystals and the 0–0 bands are somewhat intensified.[74,75] Flint and co-workers have analyzed the well-resolved $^2E \leftrightarrow {}^4A_2$ spectra from a number of Cr(III) complexes in crystals at low temperatures.[42,76-81] The relative intensities of the 0–0 and vibronic bands depend upon the distortion of the CrX_6 skeleton from centrosymmetry. This distortion is so large in $Cr(ox)_3^{3-}$ that <1% of the intensity appears in the vibronic structure.[57]

$^2E \rightarrow {}^4A_2$ emission spectra in glassy solutions often exhibit considerable structure (Figure 4).[82] In all cases a prominent 0–0 band obtains, consistent with the intraconfigurational character of this transition and the concomitant small horizontal displacements of the potential minima along all coordinates. When the chromium–ligand skeleton is centrosymmetric, e.g., $Cr(NH_3)_6^{3+}$ and *trans*-$Cr(NH_3)_4Cl_2^+$, the 0–0 band is not the most intense feature.[82,83] Vibronic transitions involving skeletal and Cr–N–H bending modes are much more intense than those associated with ligand-localized motions. If the departure from centrosymmetry is pronounced, as in *cis*-$Cr(NH_3)_4Cl_2^+$, the 0–0 band becomes dominant. As a general rule the emission from *cis*-CrN_4X_2 and $Cr(NH_3)_5X$ complexes is mainly concentrated in a single strong peak.

The emission spectra of *trans*-$CrN_4(H_2O)_2^{3+}$ complexes in alcohol–water glasses are an exception to the generalization that the 0–0 band is not the most intense

TABLE I. Hexaamine Chromium(III) Complexes at 77 K

complex	solvent[a]	$\Delta E \times 10^{-3}$, cm^{-1}	$\tau^{-1} \times 10^{-4}$, s^{-1}	ref
$Cr(NH_3)_6^{3+}$	A/W	15.2	1.47	205
	D/W	15.2	1.37[b]	114
	$[Rh(NH_3)_6]Cl_3$		1.33	206
$Cr(ND_3)_6^{3+}$	D/W	15.2	0.019, 0.018[b]	114, 138
$Cr(en)_3^{3+}$	A/W	14.9	0.90	205
	D/W	14.9	0.79[b]	114
	D/A	15.0	0.83	129
$Cr(D\text{-}en)_3^{3+}$	A/W	14.9	0.024	207
	D/W		0.021	114
$Cr(pn)_3^{3+}$	D/A	15.0	0.90	129
$Cr(tn)_3^{3+}$	D/A	15.0	0.75	129
$Cr(D\text{-}tn)_3^{3+}$	D/W		0.021[b]	114
$Cr(meam)_6^{3+}$	D/A		0.70	129
$Cr(etam)_6^{3+}$	D/A	15.1	0.71	129
$Cr(diamsar)^{3+}$	A/W	14.6	0.90	131
	CH_3CN		0.95	130
$Cr(D\text{-}diamsar)^{3+}$	CH_3CN		0.25	130
$Cr(sen)^{3+}$	D/W	14.8	0.84	132
$Cr(tacn)_2^{3+}$	D/W	14.7	0.29	114
$Cr(D\text{-}tacn)_2^{3+}$	D/W	14.7	0.031	114
$Cr(en)_2(NH_3)_2^{3+}$	D/A	15.0	1.06	129
$Cr(pn)_2(NH_3)_2^{3+}$	D/A	15.0	1.04	129
$Cr(tn)_2(NH_3)_2^{3+}$	D/A	15.1	0.91	129
$Cr(en)_2(pn)^{3+}$	D/A	15.0	0.85	129
$Cr(en)(pn)_2^{3+}$	D/A	15.0	0.85	129
$Cr(en)_2(tn)^{3+}$	D/A	14.9	0.90	129
$Cr(en)(tn)_2^{3+}$	D/A	15.0	0.83	129
$Cr(en)_2(meam)_2^{3+}$	D/A	15.0	0.91	129
$Cr(pn)_2(meam)_2^{3+}$	D/A	15.0	0.85	129
$Cr(tn)_2(meam)_2^{3+}$	D/A	15.1	0.75	129
$Cr(meam)_5(NH_3)$	D/A	15.1	0.80	129
$Cr(etam)_5(NH_3)^{3+}$	D/A	15.1	0.74	129
$Cr(D\text{-}tn)_3^{3+}$	D/W	15.0	0.020[b]	114
$Cr(dien)_2^{3+}$	D/A	14.7	1.03	129
$Cr(ditn)_2^{3+}$	D/A	15.0	0.50	129
$Cr(D\text{-}ditn)_2^{3+}$	D/W	15.0	0.024[b]	114
cis-$Cr(cyclam)(en)^{3+}$	A/W, D/A	14.7	0.74	84, 129
cis-$Cr(D\text{-}cyclam)(D\text{-}en)^{3+}$	D/W	14.8	0.045[b]	114
cis-Cr(tet*b*)(en)	D/W	14.7	1.09	206
trans-$Cr(cyclam)(NH_3)_2$	A/W	14.9	0.50	84
cis-$Cr(cyclam)(NH_3)_2$	A/W	14.9	0.89	84
trans-$Cr(D\text{-}cyclam)(ND_3)_2^{3+}$	D	14.8	0.027	184
cis-$Cr(D\text{-}cyclam)(ND_3)_2^{3+}$	D	14.8	0.063	184
trans-$Cr(teta)(NH_3)_2^{3+}$	D/W		0.47	208
$Cr(cha)_3^{3+}$	$D/CHCl_3$	14.8	1.04	18
$Cr(dtne)^{3+}$	D/W	13.7	1.99	132
$Cr(D\text{-}dtne)^{3+}$	D/W	13.7	0.88	132
$Cr(tacn)(NH_3)_3^{3+}$	D/W	15.0	0.97	132

[a] A = alcohol or polyalcohol, D = DMSO, W = H_2O or D_2O. [b] 35 K.

in trans complexes.[84] This suggests that hydrogen-bonding between the coordinated water and the solvent leads to skeletal distortion.

In contrast to the highly structured $^2E \rightarrow {}^4A_2$ phosphorescence, the fluorescence spectra are not structured at 77 K, even in crystalline media. $^4T_2 \rightarrow {}^4A_2$ emission spectra, which arise from the interconfigurational $t_2^2e \rightarrow t_2^3$ transition, are broader than the $^2E \rightarrow {}^4A_2$ bands with significant intensity over a range that exceeds 1000 cm^{-1}.[52,54] Structure is resolved in the fluorescence emission at lower temperatures.[22,23]

The well-resolved low-temperature emission spectra of crystals containing *trans*-$Cr(py)_4F_2^+$, *trans*-$Cr(en)_2F_2^+$, and $Cr(NH_3)_5OH^{2+}$ ions exhibit relatively intense features over a large interval.[37,43,85] The band envelopes of the emissions in glassy media resemble those of $^4T_2 \rightarrow {}^4A_2$ spectra in breadth.[82,86,87] However, these emissions appear at the wrong positions to be assigned as fluorescence. On the basis of crystal field calculations and the polarized absorption spectrum of *trans*-$Cr(en)_2F_2^+$,[88] Flint assigned the emission as $^2E^Q \rightarrow {}^4A_2$.[85] The emissions from the other two complexes were similarly assigned.

Since both the $^2E^Q \rightarrow {}^4A_2$ and $^4T_2 \rightarrow {}^4A_2$ transitions give rise to broad spectra in solution, the spectral appearance is not sufficient to distinguish the two transitions. Illustrative of this difficulty is the *trans*-$Cr(en)_2F_2^+$ emission, where the broad room temperature spectrum in aqueous solution was first assigned as fluorescence.[89] The wide gap between the long-wavelength tail of the $^4T_2 \rightarrow {}^4A_2$ absorption band[90] and the short-wavelength tail of the emission band casts doubt on this assignment. The low-temperature spectra indicate that the $^2T_1$ splitting is large enough in *trans*-$CrN_4F_2^+$ complexes to depress $^2E^Q$ below ^2E.[85,87] The room temperature emission might also be $^2E^Q \rightarrow {}^4A_2$.[91]

The transition energies listed in Tables I–IV correspond to the 0–0 band positions for the $^2E \rightarrow {}^4A_2$ spectra that comprise the bulk of the tabulated data. Where the emission is broad, the values refer to the $^2E^Q \rightarrow {}^4A_2$ band maxima, which lie some 500–1000 cm^{-1} to the red of the 0–0 band.

TABLE II. Non-Amine Homoliganded Chromium(III) Complexes at 77 K

complex	solvent[a]	$\Delta E \times 10^{-3}$, cm^{-1}	$\tau^{-1} \times 10^{-4}$, s^{-1}	ref
$Cr(H_2O)_6^{3+}$	A/W	14.7	<6.0	138
	D/W	14.7	6.25	136
$Cr(D_2O)_6^{3+}$	A/W	14.7	<0.2	138
	$AlCl_3 \cdot 6D_2O$	14.6	<0.3	60, 134
$Cr(ox)_3^{3-}$	A/W		0.100	60
	$NaMgAl(ox)_3 \cdot 9H_2O$	14.5	0.111	60
$Cr(acac)_3$	EPA, A/W	12.8	0.24	5
	$Al(acac)_3$	12.9	0.21	55, 32
$Cr(3\text{-}C_2H_5\text{-}acac)_3$	EPA	12.3	0.64	5
$Cr(3\text{-}NO_2\text{-}acac)_3$	EPA	12.9	0.15	5
$Cr(3\text{-}I\text{-}acac)_3$	EPA	12.3	0.90	5
$Cr(3\text{-}Br\text{-}acac)_3$	EPA	12.4	0.44	5
$Cr(3\text{-}Cl\text{-}acac)_3$	EPA	12.4	0.40	5
$Cr(2,4\text{-}(CF_3)_2\text{-}acac)_3$	EPA	12.3	1.43	5
$Cr(2,4\text{-}Ph_2\text{-}acac)_3$	EPA	12.1	1.89	5
$Cr(2\text{-}H\text{-}acac)_3$	EPA	12.6	1.09	5
$Cr(2,4\text{-}H_2\text{-}acac)_3$	EPA	12.4	2.50	5
$Cr(2\text{-}Ph\text{-}acac)_3$	EPA	12.4	0.66	5
$Cr(DMSO)_6^{3+}$	D	14.0	1.00	209
	A/W		0.5–0.7	100
$Cr(urea)_6^{3+}$	A/W	14.2	>500	58
$Cr(exan)_3$	$EPA/CHCl_3$	12.8	0.26	210
$Cr(mxan)_3$	$EPA/CHCl_3$	12.8	0.29	210
$Cr(dtc)_3$	$EPA/CHCl_3$	12.5	0.85	210
$Cr(dtmc)_3$	$EPA/CHCl_3$	12.5	0.78	210
$Cr(CN)_6^{3-}$	A/W	12.4	0.024	215
	$K_3Co(CN)_6$		0.00080	60
$Cr(oxine)_3$	EPA	13.1	2.55	5
$Cr(bpy)_3^{3+}$	A/W	13.7	0.015	211
$Cr(phen)_3^{3+}$	A/W	13.7	0.019	211
$Cr(NCS)_6^{3-}$	A/W	12.9	0.024	138
$Cr(terpyridyl)_2^{3+}$	D/W	13.0	0.185	206

[a] A = alcohol or polyalcohol, D = DMSO, W = H_2O or D_2O, EPA = ethyl ether–isopentane–ethanol (5:5:2 (v/v)).

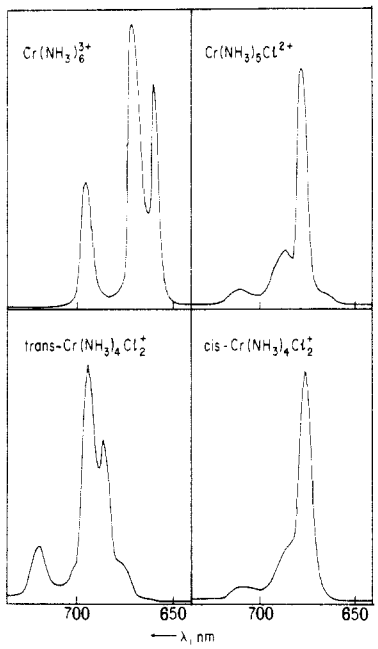

Figure 4. Representative $^2E \rightarrow {}^4A_2$ spectra of Cr(III) complexes in ethylene glycol/H_2O (2:1 (v/v)) at 77 K.

In O_h symmetry the occupation number of each t_2 orbital is unity in the ^2E and $^4A_2$ levels derived from the t_2^3 configuration.[92] The half-filled character of this configuration precludes significant Jahn–Teller distortions. The consequence of the identical electron distribution in ^2E and $^4A_2$ is a very small difference in geometry and vibrational frequencies in the two levels. When the symmetry is lowered by a tetragonal field in a CrN_4XY complex, the orbital occupation numbers are unchanged in ^2E even though the t_2 orbital set is split into two groups.[92] However, the t_2 occupation numbers are no longer equal in the $^2T_1$ components. In the case where $^2E^Q$ lies below $^2A_2^Q$, charge is drawn from the antibonding axial orbitals and the Cr–X bond is shortened. The geometry difference between the ground and emitting states leads to a spectrum in which many vibronic bands are relatively intense. According to a Franck–Condon analysis, based on a progression in the totally symmetrical stretching modes, the Cr–F bond is 0.01 nm shorter in $^2E^Q$ than in the ground state.[43] In solution, multiple solvates lead to a blurring of the vibronic structure, and a broad emission band is the result.

The $^2T_1$ degeneracy is also reduced in trigonal fields but, in contrast to the quadrate field case, no $^2T_1$ component is expected to lie below ^2E.[94] The t_2 orbital occupation in ^2E is no longer uniform in trigonal complexes.[93] Ceulemans et al. suggest that the geometry changes associated with the unequal orbital distribution could lead to broad $^2E \rightarrow {}^4A_2$ spectra in trigonal complexes. However, the emission of $Cr(acac)_3$ is very narrow in dilute crystals,[32,33] and the spectra of $Cr(en)_3^{3+}$ and $Cr(bpy)_3^{3+}$ in glasses resemble the usual $^2E \rightarrow {}^4A_2$ emissions. The lowest level in $Cr(acac)_3$ has been identified as a $^2T_1$ component on the basis of Zeeman splittings.[34] If this is correct, neither ligand field theory nor the AOM model can explain this level ordering.

The large $^2T_1$ splittings that force $^2E^Q$ below ^2E in *trans*-$CrN_4F_2^+$ complexes are qualitatively consistent with the AOM parameters extracted from the fitting of the spin-allowed absorption bands in *trans*-CrN_4X_2 complexes.[46] The π-donation parameters decrease in

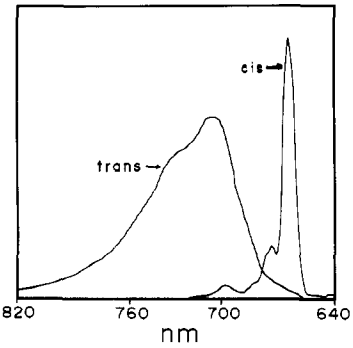

Figure 5. Emission spectra of the $Cr(NH_3)_4F_2^+$ isomers in ethylene glycol/H_2O (2:1 (v/v)) at 77 K.

the order $OH^- > F^- > H_2O > Cl^- > Br^- > NH_3 >$ py. According to the AOM $\Delta(t_2)$ should be twice as large in a trans complex as in the cis analogue. The $^2T_1$ splitting would then be largest in *trans*-$CrN_4(OH)_2^+$ and *trans*-$CrN_4F_2^+$ complexes. It is these species that exhibit the broad $^2E^Q \rightarrow {}^4A_2$ bands in alcohol–water glasses while the emission from the cis counterparts is $^2E \rightarrow {}^4A_2$ in the same media (Figure 5).[82,87] The AOM fitting of the spin-allowed absorption bands of *trans*-$Cr(py)_4X_2$ complexes suggests that the pyridine π-donation parameter is negative.[46] The assignment of the AOM parameters to individual ligands requires the assumption that the parameters are transferable from one complex to another. The putative negative value of the pyridine π-parameter has been questioned,[95,96] but this interpretation has proven to be useful for the classification of some of the emission spectra. In particular, the emission change from $^2E^Q \rightarrow {}^4A_2$ in alcohol–water glasses of *trans*-$Cr(py)_4(H_2O)_2^{3+}$ and *cis*-$Cr(bpy)_2(OH)_2^+$ to $^2E \rightarrow {}^4A_2$ in the corresponding NH_3 complexes[86,87] indicates that the $^2T_1$ splitting is increased when NH_3 is replaced by either py or bpy. The solvent effects on the emission spectra of *cis*-$Cr(NH_3)_4F_2^+$, *cis*-$Cr(phen)F_2^+$, and *cis*-$Cr(bpy)_2F_2^+$ are in accord with the supposition that the π parameter is negative for pyridine and polypyridine ligands.[86,87] Ryu and Endicott also assigned a negative π parameter to bpy and phen.[97] It must be borne in mind that vibronic interactions are omitted in the AOM and ligand field treatments. The proximity of ^2E and $^2T_1$ would lead to significant vibronic mixing, and the ^2E and $^2E^Q$ labels provide only a crude description.

The emission spectral breadth at 12 K varies considerably within a group of tris amino carboxylate complexes.[98] The broad emission bands were assigned as $^4T_2 \rightarrow {}^4A_2$, but neither the Schläfer rule nor the relative shifts of the emission bands and the corresponding $^4T_2 \leftarrow {}^4A_2$ absorption bands with ligand support this assignment. These emission spectra may be $^2E \rightarrow {}^4A_2$ and the spectral breadth due to the geometrical distortions induced by the charge anisotropy.[92] The low-temperature crystal emission spectra of several amino carboxylate complexes with CrN_2O_4 skeletons, *cis*-$Cr(ida)_2^-$ and *trans*-$Cr(mida)_2^-$, and $^2E^Q \rightarrow {}^4A_2$.[99] In contrast, the emission of *trans*-$Cr(pdc)_2^-$, where the nitrogen coordination involves pyridine, is $^2E \rightarrow {}^4A_2$. The red shift of the narrow *trans*-$Cr(pdc)_2^-$ band to 784 nm indicates substantial π delocalization induced by the near planarity of the pyridine moieties. The broad band at 77 K in $Na[Cr(mida)_2]$ has been assigned as thermally induced fluorescence.[99]

C. Environmental Effects

Low-temperature emission spectra of Cr(III) complexes have been recorded in a variety of media ranging from pure and dilute crystals to glasses and frozen solvents. The $^2E \rightarrow {}^4A_2$ spectral positions and shapes often do not change appreciably with the host. Exemplarary of this invariance is *trans*-$Cr(en)_2Cl_2^+$, where the 0–0 bands in an alcohol–water glass and crystalline *trans*-$[Ir(en)_2Cl_2]Cl$ differ by <2 nm.[100] The change in the $Cr(NH_3)_6^{3+}$ ^2E energy with lattice does not exceed 100 cm^{-1},[78,83] but the host can affect the ^2E energy in $Cr(D_2O)_6^{3+}$ by as much as 500 cm^{-1}.[101]

The three narrow lines in the 4 K spectrum of dilute Cr^{3+}:$Al(acac)_3$ that span 15 cm^{-1} have been ascribed to multiple sites.[33,34] In pure $Cr(acac)_3$, the emission is broad and highly structured due to intermolecular interactions.[102] This type of broadening is not confined to complexes with ligands that delocalize the d electrons sufficiently to induce exciton splittings since a similar phenomenon has been found in crystals containing $Cr(urea)_6^{3+}$ at high concentrations.[103] Lattice effects on the ^2E splitting have also been identified in $Cr(ox)_3^{3-}$, where there is a reduction of this splitting from 20 cm^{-1} in Cr^{3+}:$NaMgAl(ox)_3 \cdot 9H_2O$ to 2 cm^{-1} when some of the hydration water is removed.[104] A 115-cm^{-1} ^2E splitting has been claimed for $Cr(ox)_3^{3-}$ in a crystalline host.[105] Also, the energy baricenters of the ^2E levels span a range of 84 cm^{-1} when $Cr(ox)_3^{3-}$ is diluted into 13 different crystalline hosts.[106,107]

The sensitivity of the $^2E^Q$ energy to solvent stands in sharp contrast to the near constancy of the ^2E energy.[86,87] $^2E^Q$ is raised when solvent–solute interactions decrease $\Delta(t_2)$. Hydrogen bonding to F^-, OH^-, and H_2O ligands is an example of such an interaction. When the $^2T_1$ splitting is large enough to depress $^2E^Q$ below ^2E, as in an alcohol–water solution of *trans*-$Cr(py)_4F_2^+$, the effect of changing the solvent to DMF is to red shift the broad $^2E^Q \rightarrow {}^4A_2$ emission. Conversely, if the $^2T_1$ splitting is small, $^2E^Q$ is above ^2E in all solvents and there will be little solvent effect on the emission spectrum. For intermediate $^2T_1$ splittings, e.g., *cis*-$Cr(phen)_2F_2^+$, a level inversion occurs: the emission is $^2E^Q \rightarrow {}^4A_2$ in DMF and $^2E \rightarrow {}^4A_2$ in alcohol–water.

The spectra of $Cr(bpy)_2(NCS)_2^+$ and $Cr(phen)_2(NCS)_2^+$ are narrow in DMF and broad in DMSO/H_2O.[97] This may be another example of ^2E–$^2E^Q$ level inversion, but the change in the $^2E^Q$ energy is not due to disruption of hydrogen bonds in these complexes.

All of the systems described above are rigid. If there is a difference in the equilibrium solute–solvent interactions in the ground and lowest excited state, the emission spectrum will be red shifted when the solvent is changed from rigid to fluid. Except for thermal population effects, $^2E \rightarrow {}^4A_2$ emission spectra are independent of solvent rigidity unless a nearby $^2E^Q$ level energy is changed when the solvent becomes fluid. On the other hand, there is a red shift of the $^2E^Q \rightarrow {}^4A_2$ band when strong solvent–solute interactions are reduced by solvent motions, e.g., *trans*-$Cr(py)_4F_2^+$.[91] This has been ascribed to an increase in $\Delta(t_2)$ that leads to a lowering of $^2E^Q$. In alcohol–water solutions of *cis*-$Cr(phen)_2F_2^+$, level inversion occurs during the rigid–fluid transition.

Adamson has emphasized the role of solvent motions in excited-state photoprocesses and has coined the term

TABLE III. Amine Heteroliganded Chromium(III) Complexes at Low Temperatures

complex	solvent[a]	$\Delta E \times 10^{-3}$,[b] cm^{-1}	$\tau^{-1} \times 10^{-4}$, s^{-1}	ref
$Cr(NH_3)_5(NCS)^{2+}$	A/W	14.5	1.43	138
$Cr(ND_3)_5(NCS)^{2+}$	D/W		0.031	137
trans-$Cr(NH_3)_4(NCS)_2^+$	A/W	13.9	0.71	138
trans-$Cr(ND_3)_4(NCS)_2^+$	D/W		0.040	137
cis-$Cr(NH_3)_4(NCS)^{2+}$	D/W	14.2	0.81	137
cis-$Cr(ND_3)_4(NCS)^{2+}$	D/W	14.1	0.040	132, 137
$Cr(NH_3)_3(NCS)_3$	A/W	13.6	0.63	138
trans-$Cr(NH_3)_2(NCS)_4^-$	A/W	13.2	0.29	138
trans-$Cr(ND_3)_2(NCS)_4^-$	D/W		0.045	137
Cr(tacn)$(NCS)_3$	D/W	13.3	0.91	132
trans-Cr(cyclam)$(NCS)_2^+$	D/A	14.6	0.55	132
cis-Cr(cyclam)$(NCS)_2^+$	D/W	13.7	1.05	132
cis-Cr(tet*b*)$(NCS)_2^+$	D/A	13.8	1.8	206
trans-Cr(teta)$(NCS)_2^+$	D/A	14.1	<0.92	206
$Cr(NH_3)_5(H_2O)^{3+}$	A/W	15.0	1.96	138
trans-$Cr(NH_3)_4(H_2O)_2^{3+}$	A/W	15.0	2.50	138
cis-$Cr(NH_3)_4(H_2O)_2^{3+}$	A/W	15.0	2.38	138
fac-$Cr(NH_3)_3(H_2O)_3^{3+}$	A/W	15.0	2.94	212
mer-$Cr(NH_3)_3(H_2O)_3^{3+}$	A/W	15.0	2.94	212
trans-$Cr(NH_3)_2(H_2O)_4^{3+}$	A/W	15.0	3.57	212
cis-$Cr(NH_3)_2(H_2O)_4^{3+}$	A/W	15.0	3.45	212
$Cr(NH_3)(H_2O)_5^{3+}$	A/W	15.0	4.54	212
$Cr(ND_3)_5(D_2O)^{3+}$	A/W	15.0	0.028	138
trans-$Cr(ND_3)_4(D_2O)_2^{3+}$	A/W	15.0	0.043	138
cis-$Cr(ND_3)_4(D_2O)_2^{3+}$	A/W	15.0	0.041	138
$Cr(ND_3)_5(H_2O)^{3+}$	A/W	15.0	0.16	138
trans-$Cr(ND_3)_4(H_2O)_2^{3+}$	A/W	15.0	0.63	138
cis-$Cr(ND_3)_4(H_2O)_2^{3+}$	A/W	15.0	0.38	138
$Cr(NH_3)_5(D_2O)^{3+}$	A/W	15.0	1.75	138
trans-$Cr(NH_3)_4(D_2O)_2^{3+}$	A/W	15.0	1.89	138
cis-$Cr(NH_3)_4(D_2O)_2^{3+}$	A/W	15.0	1.92	138
trans-$Cr(NH_3)_2(D_2O)_4^{3+}$	A/W	15.0	1.00	138
trans-$Cr(en)_2(H_2O)_2^{3+}$	A/W	14.9	1.37	205
cis-$Cr(en)_2(H_2O)_2^{3+}$	A/W	14.9	1.61	205
trans-Cr(cyclam)$(H_2O)_2^{3+}$	A/W	14.8	0.79	84
trans-Cr(cyc*a*)$(H_2O)_2^{3+}$	A/W	14.7	0.80	84
cis-Cr(cyclam)$(H_2O)_2^{3+}$	A/W	14.4	1.35	84
cis-Cr(cyc*b*)$(H_2O)_2^{3+}$	A/W	14.3	2.38	84
Cr(tacn)$(H_2O)_3^{3+}$	D/W	14.8	1.55	132
$Cr(NH_3)_5F^{2+}$	A/W	15.1	2.17	205
trans-$Cr(NH_3)_4F_2^+$	A/W	14.1*	2.04	205
cis-$Cr(NH_3)_4F_2^+$	A/W	15.1	2.86	205
trans-$Cr(en)_2F_2^+$	A/W	12.9*	2.86	205
trans-Cr(D-en)$_2F_2^+$	A/W		0.32	213
cis-$Cr(en)_2F_2^+$	A/W	14.8	1.92	205
trans-Cr(cyc*a*)F_2^+	A/W	12.7*	1.5–2.0	83
trans-Cr(teta)F_2^+	A/W		2.04	213
trans-Cr(D-teta)F_2^+	A/W		0.080	213
trans-Cr(cyclam)F_2^+	D/W	12.7	1.5–1.9	84
cis-Cr(cyclam)F_2^+	A/W	14.6	1.11	84
cis-Cr(cyc*b*)F_2^+	A/W	14.6	1.9–2.1	84
$Cr(NH_3)_5Cl^{2+}$	A/W	14.8	2.50	205
	D/W		2.08	136
trans-$Cr(NH_3)_4Cl_2^+$	A/W	14.5	3.0–3.6	205
	D/W		3.70	136
cis-$Cr(NH_3)_4Cl_2^+$	A/W	14.8	2.94	205
trans-$Cr(en)_2Cl_2^+$	A/W	14.3	2.00	205
cis-$Cr(en)_2Cl_2^+$	A/W	14.4	2.50	205
trans-$Cr(en)_2Cl_2^+$	[*trans*-$Ir(en)_2Cl_2$]Cl	14.3	1.5–2.0	100
cis-$Cr(en)_2Cl_2^+$	[*cis*-$Ir(en)_2Cl_2$]Cl·H_2O	14.3	3.45	100
trans-Cr(cyclam)Cl_2^+	A/W	14.3	1.15	84
trans-Cr(teta)Cl_2^+	D/W	14.4	1.06	206
cis-Cr(cyclam)Cl_2^+	A/W	14.2	2.10	84
cis-Cr(tet*b*)Cl_2^+	D/W		1.06	84
$Cr(NH_3)_5Br^{2+}$	A/W	14.8	1.85	205
trans-$Cr(en)_2Br_2^+$	A/W	14.2	1.0–1.3	205
cis-$Cr(en)_2Br_2^+$	A/W	14.2	1.5	205
$Cr(NH_3)_5CN^{2+}$	A/W	14.7	1.00	100
$Cr(ND_3)_5CN^{2+}$	D/W	14.7	0.013	132
trans-$Cr(en)_2(CN)_2^+$	D		0.48	140
cis-$Cr(en)_2(CN)_2^+$	D		0.50	140
cis-Cr(D-en)$_2(CN)_2^+$	D		0.033	140
trans-Cr(teta)$(CN)_2^+$	D/A	14.3	0.26	18, 206
	D/W		0.18	208
trans-Cr(D-teta)$(CN)_2^+$	D/A	14.3	0.018	18
cis-Cr(tet*b*)$(CN)_2^+$	D/A	13.8	0.48	18, 206
cis-Cr(D-tet*b*)$(CN)_2^+$	D/A	13.8	0.054	18

TABLE III (Continued)

complex	solvent[a]	$\Delta E \times 10^{-3}$,[b] cm^{-1}	$\tau^{-1} \times 10^{-4}$, s^{-1}	ref
trans-$Cr(cyclam)(CN)_2^+$	D/W	13.9	0.20	208
trans-$Cr(teta)(CN)_2^+$	D/W	14.3	0.18	208
trans-$Cr(D\text{-}teta)(CN)_2^+$	D/W		0.018	132
trans-$Cr(D\text{-}cyclam)(CN)_2^+$	D	14.0	0.033	132, 140
$Cr(tacn)(CN)_3$	D/W	13.5	0.26	132
$Cr(NH_3)_5(OH)^{2+}$	A/W	14.3*	3.70	205
trans-$Cr(NH_3)_4(OH)_2^+$	A/W	13.6*	11–16	205
cis-$Cr(NH_3)_4(OH)_2^+$	A/W	14.6	3.27	205
trans-$Cr(en)_2(OH)_2^+$	A/W	13.3	7	205
cis-$Cr(en)_2(OH)_2^+$	A/W	14.4	2.94	205
cis-$Cr(cyclam)_2(OH)_2^+$	A/W	13.8	3.7–4.5	100
$Cr(NH_3)_5(DMSO)^{3+}$	A/W	15.0	2.27	100
cis-$Cr(NH_3)_4(DMSO)_2^{3+}$	A/W	14.9	2.50	100
$Cr(NH_3)_5(NO_3)^{2+}$	A/W		2.00	100
$Cr(NH_3)_5ONO^{2+}$	A/W	14.8	4.17	205
$Cr(NH_3)_5(OCOR)^{2+}$ (R = CF_3, CCl_3, $CHCl_2$, CH_2Cl, CH_3)	D/A	15.5	1.79	214
$Cr(en)(ox)_2^-$	A/W	14.4	1.09	100
$Cr(D\text{-}en)(ox)_2^-$	D/W		0.06–0.09	207
$Cr(en)_2ox^+$	A/W	14.6	1.14	100
$Cr(D\text{-}en)_2ox^+$	D/W		0.040	207
$Cr(NH_3)_4ox^+$	A/W	14.8	1.73	100
trans-$Cr(NH_3)_4(H_2O)(OH)^{2+}$	A/W	13.8	7–8	205
trans-$Cr(en)_2(H_2O)(OH)^{2+}$	A/W	13.0	10–14	205
cis-$Cr(en)_2(OH)F^+$	A/W	14.5	2.94	205
trans-$Cr(en)_2ClF^+$	A/W	13.9	1.0–1.2	205
cis-$Cr(en)_2ClF^+$	A/W	14.5	2.08	205
trans-$Cr(en)_2(H_2O)F^{2+}$	A/W	13.8	1.49	205
cis-$Cr(en)_2(H_2O)F^{2+}$	A/W	14.7	1.92	205
trans-$Cr(NH_3)_4(H_2O)Cl^{2+}$	A/W	14.7	3.33	205
	D/W		2.56	136
cis-$Cr(NH_3)_4(H_2O)Cl^{2+}$	A/W	14.8	3.00	205
	D/W		2.17	136
Cr(tcta)	D/W	14.0	0.254	132
trans-$Cr(NH_3)_4(OH)Cl^+$	A/W	14.0	4.00	205
cis-$Cr(NH_3)_4(OH)Cl^+$	A/W	14.6	3.45	205
cis-$Cr(NH_3)_2(phen)_2^{3+}$	D/W	14.2	0.52	132
$Cr(en)_2(bpy)^{3+}$	D/W	14.4	0.62	132
$Cr(en)_2(phen)^{3+}$	D/W	14.4	0.65	132

[a] A = alcohol or polyalcohol, D = DMSO, W = H_2O or D_2O. [b] 0–0 band when resolved: otherwise band maximum (*).

thexi state to describe the situation in which the electronically excited complex behaves as a new species with well-defined thermodynamic properties.[108] Differences in the thexi-state energies in rigid and fluid media depend on the relative values of the correlation times for solvent motion and the excited-state lifetime in the rigid and fluid environments. There will always be a temperature range where the thexi description fails and dynamical processes dominate.

The possibility of impurity emission must never be overlooked. This is especially true when the complex is embedded in a crystalline environment. A case in point is the broad emission originally reported for pure $[Cr(NH_3)_5Cl]Cl_2$.[109] The position and shape of the spectrum suggest a $^2E^Q \rightarrow {}^4A_2$ assignment. Since the emission of $Cr(NH_3)_5Cl^{2+}$ is $^2E \rightarrow {}^4A_2$ in a glassy solution, this would require a ^2E–$^2E^Q$ level inversion between the crystalline and glassy environments. However, recent work has shown that the crystal emission is $^2E \rightarrow {}^4A_2$[40] and that the earlier result was spurious. A marked difference in the emission of *trans*-$Cr(cyclam)(CN)_2^+$ in crystals and glasses has been reported.[110] The experience with $Cr(NH_3)_5Cl^{2+}$ suggests caution in accepting this result.

D. The Nephelauxetic Effect

According to ligand field theory the ^2E energy is independent of Dq and the $^2E \rightarrow {}^4A_2$ transitions for many Cr(III) complexes are observed in the wavelength region 660–700 nm. There are a number of examples, however, in which this transition is shifted to substantially longer wavelengths. This lowering of the ^2E energy, which is ascribed to reduction of the interelectronic repulsion between the d electrons, has been called the nephelauxetic effect. Large decreases in ^2E are induced by ligands with low-lying π^* antibonding orbitals that decrease electron repulsion by delocalizing the d electrons onto the ligands. The emissions from $Cr(CN)_6^{3-}$ and $Cr(acac)_3$ occur near 800 nm. Smaller nephelauxetic shifts prevail in $Cr(NCS)_6^{3-}$, $Cr(bpy)_3^{3+}$, and $Cr(oxine)_3$. In $CrA_{6-n}B_n$ complexes with delocalizing ligands, e.g., $Cr(NH_3)_{6-n}(NCS)_n^{(3-n)}$, the wavelength of the emission maximum increases monotonically with n. Similarly, the emission of $Cr(pic)_3^{3+}$, where the coordination is by both amine and pyridine ligands, is intermediate in position between the bands of the homoliganded amine and pyridine complexes.[111]

The emission of complexes with sulfur coordination also indicates a large nephelauxetic shift (Table III).

In using the Table I data for estimating nephelauxetic effects, it is essential to distinguish the ΔE values that refer to the 0–0 bands for the sharp $^2E \rightarrow {}^4A_2$ transitions from those that correspond to the band maxima of the broad $^2E^Q \rightarrow {}^4A_2$ transitions. In the latter cases the large Stokes shifts usually lead to emission beyond 700 nm. The ^2E and $^2T_1$ energies are both dependent upon d-electron repulsion and one would expect the nephe-

TABLE IV. Miscellaneous Heteroliganded Chromium(III) Complexes at Low Temperatures

complex	solvent[a]	$\Delta E \times 10^{-3}$,[b] cm^{-1}	$\tau^{-1} \times 10^{-4}$, s^{-1}	ref
$Cr(DMSO)_5(NCS)^{2+}$	D	13.9	0.83	209
$Cr(DMSO)_4(NCS)_2^{+}$	D	13.7	0.40	209
$Cr(DMSO)_3(NCS)_3$	D	13.5	0.20	209
$Cr(DMSO)_2(NCS)_4^{-}$	D	13.2	0.100	209
$Cr(DMSO)(NCS)_5^{2-}$	D	13.0	0.045	209
$Cr(CN)_5(H_2O)^{2-}$	A/W	12.9	0.05	215
$Cr(CN)_4(H_2O)_2^{-}$	A/W	13.3	0.44–0.67	215
$Cr(CN)_3(H_2O)_3$	A/W	13.7	0.55	215
$Cr(CN)_2(H_2O)_4^{+}$	A/W	14.1	0.91	215
$Cr(CN)(H_2O)_5^{2+}$	A/W	14.6	1.81	215
cis-$Cr(bpy)(ox)_2^{-}$	A/W	13.7	0.065	100
trans-$Cr(py)_4F_2^{+}$	A/W	12.4*	0.50	86
cis-$Cr(phen)_2F_2^{+}$	A/W	13.7	0.05–0.11	86
	DMF	12.8*	0.10–0.35	86
trans-$Cr(py)_4(H_2O)_2^{3+}$	A/W	13.2*	>1	86
trans-$Cr(py)_4(D_2O)_2^{3+}$	A/W	13.2*	0.14–0.20	86
cis-$Cr(bpy)_2(H_2O)_2^{3+}$	A/W	14.1	0.313	86
cis-$Cr(bpy)_2(D_2O)_2^{3+}$	A/W	14.1	0.045	86
trans-$Cr(py)_4Br_2^{+}$	A/W	13.9	0.042	86
trans-$Cr(py)_4ClF^{+}$	A/W	13.6	0.133	100
trans-$Cr(py)_4FBr^{+}$	A/W	13.4	0.14	100
cis-$Cr(bpy)_2Cl_2^{+}$	A/W	13.2	0.095	100
trans-$Cr(py)_4Cl_2^{+}$	A/W	13.7	0.049	100
cis-$Cr(bpy)_2F_2^{+}$	A/W	13.6	0.100	100
cis-$Cr(bpy)_2(OH)_2^{+}$	A/W	13.2*	2.2–3.2	100
cis-α-$Cr(pic)_2F_2^{+}$	A/W	1.43	0.59	111
cis-α-$Cr(pic)_2Cl_2^{+}$	A/W	1.40	0.61	111
cis-β-$Cr(pic)_2Cl_2^{+}$	A/W	1.40	0.50	111
cis-α-$Cr(pic)_2Br_2^{+}$	A/W	1.39	0.43	111
fac-$Cr(pic)_3^{3+}$	A/W	14.4	0.54	111
mer-$Cr(pic)_3^{3+}$	A/W	14.2	0.47	111
$Cr(phen)_2(NCS)_2^{+}$	D/W	12.6	0.13	97
$Cr(bpy)_2(NCS)_2^{+}$	D/W	12.6	0.15	97
$Cr(phen)(CN)_4^{-}$	D/W	12.8	0.023	97
$Cr(bpy)_2(CN)_2^{+}$	D/W	13.2	0.028	97
$Cr(4,7\text{-}Ph_2phen)_3^{3+}$	D/W	13.5	0.029	132
$Cr(4,7\text{-}Me_2phen)_3^{3+}$	D/W	13.6	0.017	132
$Cr(5\text{-}Clphen)_3^{3+}$	D/W	13.7	0.19	132
trans-$Cr(pdc)_2^{-}$	A/W	12.8	0.44	189

[a] A = alcohol or polyalcohol, D = DMSO, W = H_2O or D_2O. [b] 0–0 band when resolved; otherwise band maximum (*).

lauxetic effect to shift the $^2E^Q \rightarrow {}^4A_2$ band to the red also. In the absence of information about the band origins, it is difficult to compare directly the nephelauxetic shifts for broad and sharp emissions. In addition, as discussed above, the $^2E^Q$ energy can be quite solvent dependent, further compounding the uncertainties.

Electron delocalization onto the ligands with π-acceptor orbitals is not the only way in which the nephelauxetic effect arises. In complexes with amine coordination the emission moves progressively to the red in the sequence NH_3 < en < cyclam.[84] This shift, which seems to be related to the number of NH bonds in the directly coordinated nitrogen atoms, is smaller than the nephelauxetic effect associated with ligand π orbitals. Illustrative of this phenomenon is the movement of the $^2E \rightarrow {}^4A_2$ transition from 688 nm in *trans*-$Cr(NH_3)_4Cl_2^{+}$ to 701 nm in *trans*-$Cr(cyclam)Cl_2^{+}$.

There are long-lived emissions near 850 nm in Cr(III) porphyrin complexes.[112,113] These might be due to highly delocalized $^2E \rightarrow {}^4A_2$ transitions but they have been assigned as ligand-localized triplet → singlet transitions enhanced by coupling with the d electrons in much the same way as the visible absorption bands in $Cr(acac)_3$ and $Cr(bpy)_3^{3+}$ are intensified.[20] The coupling of the ligand triplet to $^4T_2$ leads to sextet, quartet, and doublet levels and the low-temperature emission from the porphyrin complexes was classified as sextet → quartet in the spin designation appropriate to the entire complex. This interpretation is supported by the appearance of thermally activated quartet → quartet emission at 815 nm.

IV. Excited-State Relaxation

A. Kinetic Analysis

Depending upon the excitation wavelength, the initially populated vibronic level can be in the quartet or doublet manifold. Absorption is normally into one of the relatively intense spin-allowed bands. It is sufficient for kinetic purposes to imagine excitation into a high vibrational level of $^4T_2$. A number of processes can then ensue (Figure 1). In particular, vibrational relaxation within $^4T_2$ competes with intersystem crossing. Without loss of generality it can be assumed that ^2E is the lowest doublet level. If a thermalized vibrational distribution in ^2E is achieved before significant depopulation of that level occurs, the ^2E concentration following δ-function excitation is described by

$$[^2E] = (a_1 \exp(-\lambda_1 t) + a_2 \exp(-\lambda_2 t))/(\lambda_2 - \lambda_1) \quad (1)$$

where $\lambda_{1,2} = 0.5[(k_E + k_T) \mp ((k_T - k_E)^2 + 4k_4k_{-4})^{1/2}]$, $k_E = k_5 + k_6 + k_{-4}$, $k_T = k_2 + k_3 + k_4$, $a_1 = [^4T_2]_0k_4 + [^2E]_0(\lambda_2 - k_E)$, $a_2 = -[^4T_2]_0k_4 + [^2E]_0(k_E - \lambda_1)$, $[^4T_2]_0 = (1 - \eta_{pisc} - \eta_{pr})I_{abs}$, and $[^2E]_0 = \eta_{pisc}I_{abs}$. $[^4T_2]_0$ and $[^2E]_0$ represent thermalized distributions at $t = 0$, and η_{pisc} and η_{pr} are the fractions of the initially excited molecules in $^4T_2$ that crossover to ^2E or react in $^4T_2$ prior to achievement of a Boltzmann vibrational distribution in that level; i.e., $[^4T_2]_0 + [^2E]_0 = I_{abs}(1 - \eta_{pr})$. Processes that occurs in thermalized $^4T_2$ are designated by k_2, k_3, and k_4 while the corresponding processes in thermalized ^2E are described by k_{-4}, k_5, and k_6. Reactions that depopulate $^4T_2$ and ^2E are included in k_3 and k_6, respectively.

The time evolution of the $^4T_2$ population is given by

$$[^4T_2] = (a_3 \exp(-\lambda_1 t) + a_4 \exp(-\lambda_2 t))/(\lambda_2 - \lambda_1) \quad (2)$$

with $a_3 = [^4T_2]_0(\lambda_2 - k_T) + [^2E]_0k_{-4}$ and $a_4 = [^4T_2]_0(-\lambda_1 + k_T) - [^2E]_0k_{-4}$. If $k_{-4} = 0$, $\lambda_1 = k_E$, $\lambda_2 = k_T$, and the measured ^2E lifetime is $\tau = \lambda_1^{-1}$. When k_{-4} is not negligible, the decay rate at long times is λ_1 for both $^2E \rightarrow {}^4A_2$ and $^4T_2 \rightarrow {}^4A_2$ emission.

Equation 1 describes the decay from a collection of excited molecules in identical environments. In principle, a nonexponential decay will be observed, but if $\lambda_2 \gg \lambda_1$ the decay will be exponential for $t \gg \lambda_2^{-1}$. If more than one level is populated, e.g., ^2E and $^2T_1$, exponentiality still obtains as long as a Boltzmann distribution is maintained between the several excited levels. The measured decay rate is then a population weighted average of the decay rates from the individual levels. When multiple environments with different decay rates are present, the decay will be exponential only if the interconversion rates between the environments are large compared to the excited-state relaxation rates.

Three types of systems are involved in decay measurements of Cr(III) complexes: pure crystals, dilute crystals, and solutions. Data from pure crystals are

TABLE V. Radiative Rates for $^2E \rightarrow {}^4A_2$ at Low Temperatures in Crystalline Hosts

system	k_5,[a] s^{-1}	ref	τ^{-1}, s^{-1}	ref
Cr^{3+}:MgO	10	216	86	216
Cr^{3+}:$MgAl_2O_4$	4	217	27	217
$Cr(CN)_6^{3-}$:$K_3Co(CN)_6$	25[b]	60	8	60
$Cr(ox)_3^{3-}$:$NaMgAl(ox)_3 \cdot 9H_2O$	>150	27, 119	1111	60
Cr^{3+}:Al_2O_3	213	25	239	25
$Cr(acac)_3$:$Al(acac)_3$	115	56	2326	60
$Cr(D_2O)_6^{3+}$:GASD[c]	7	60, 118	667	60
$Cr(D_2O)_6^{3+}$:$AlCl_3 \cdot 6D_2O$	17	60	2860	60

[a] Calculated from $k_5 = (n^2 f \bar{\nu}^2)/1.51$, with f estimated from the total $^2E \leftarrow {}^4A_2$ absorption or from the oscillator strength in the R lines and the fraction of the emission concentrated in the R lines. [b] Calculated from the low-temperature absorption of pure $K_3Co(CN)_6$. [c] GASD = $C(NH_2)_3Al(SO_4)_2 \cdot 6D_2O$.

suspect because decay rates are susceptible to crystal imperfections and intermolecular interactions. An isostructural host can provide a unique environment for the dispersed complex, e.g., $Cr(D_2O)_6^{3+}$:$AlCl_3 \cdot 6D_2O$,[60] but multiple sites can lead to nonexponentiality.[58] It is remarkable that the multiple environments existing in a rigid glass solution do not always lead to significant nonexponentiality. As measurement techniques improve, smaller deviations from exponentiality can be detected. In the older literature most of the decay curves were recorded by photographing oscilloscope traces, but digital techniques involving signal averaging are now routine. Consequently, there is a variation in data quality for the reported lifetimes. Differences in decay rates are often interpretable even when there is some nonexponentiality, and the extant data are listed in Tables I–IV without regard to the degree of exponentiality.

B. Radiative Rates

The most fundamental method for the measurement of the radiative rate, k_5, involves the determination of the oscillator strength of the 0–0 transition (f_R) in absorption. The total oscillator strength of the $^2E \leftarrow {}^4A_2$ transition is then calculated from $f = f_R/\eta_R$, where η_R is the fraction of the emission intensity concentrated in the R lines.[25] The radiative rate is related to f by

$$k_5 = n^2 f \bar{\nu}^2 / 1.51 \quad (3)$$

where $\bar{\nu}$ is the transition energy in cm^{-1} and n the refractive index. The accurate evaluation of f_R at low temperatures has been made only for a few single crystals. A similar, but less reliable method, has been applied to complexes in solution.[114-116] In this approach the oscillator strength is calculated from $f = 4.31 \times 10^{-9} \int \epsilon(\bar{\nu})\, d\bar{\nu}$. When room temperature absorption data in solution are used to calculate the radiative rates, the computed values will be larger than those calculated from the low-temperature oscillator strengths. The computed k_5 are compared to τ^{-1} in Tables V and VI.

An alternative procedure involves the use of the equation

$$\Phi_p/\tau = \eta_D k_5 \quad (4)$$

where Φ_p is the absolute quantum yield of emission, a difficult quantity to evaluate,[117] and η_D is the total intersystem crossing efficiency, both prompt and from a thermalized $^4T_2$ distribution. Although η_D cannot exceed unity, the exact values are elusive quantities.

TABLE VI. Radiative Rates for $^2E \rightarrow {}^4A_2$ in Noncrystalline Hosts

	k_5,[a] s^{-1}		τ^{-1}, s^{-1}	Φ_p/τ, s^{-1} ref 114	
complex	ref 114	ref 115	ref 114[b]	295 K	35 K
$Cr(NH_3)_6^{3+}$	130	140		11.9	42.5
$Cr(ND_3)_6^{3+}$	149		175	13.8	29.8
$Cr(en)_3^{3+}$	192	312		24.0	70.9
$Cr(D\text{-}en)_3^{3+}$	192		208	35.0	50.0
$Cr(tn)_3^{3+}$	143	213		20.3	45.7
$Cr(D\text{-}tn)_3^{3+}$	164		208	22.3	54.2
$Cr(ditn)_2^{3+}$	213			35.9	71.4
$Cr(D\text{-}ditn)_2^{3+}$	196		294	51.4	102.4
Cr(cyclam)en^{3+}	357			83.6	126.8
Cr(D-cyclam)D-en^{3+}			454	77.5	145
$Cr(tacn)_2^{3+}$	185			28.5	79.4
$Cr(D\text{-}tacn)_2^{3+}$			313	26.6	84.4
$Cr(pn)_3^{3+}$		730			
$Cr(NH_3)_5F^{2+}$		246			
$Cr(NH_3)_5Cl^{2+}$		100			
$Cr(NH_3)_5Br^{2+}$		128			
$Cr(CN)_6^{3-}$		97			
$Cr(NCS)_6^{3-}$		302			
$Cr(ox)_3^{3-}$		625			
$Cr(bpy)_3^{3+}$		182			
$Cr(phen)_3^{3+}$		319			

[a] Calculated from $2.88 \times 10^{-9} n^2 \bar{\nu}^2 \int \epsilon(\bar{\nu})\, d\bar{\nu}$, with ϵ the 295 K molar absorption and $n = 1.4$. [b] 35 K.

Several Φ_p/τ values are included in Table VI.

The very small k_5 value in Cr^{3+}:MgO for ions in O_h sites is due to the magnetic dipole nature of the transition.[21] Likewise, the spectrum of $Cr(CN)_6^{3-}$:$K_3Co(CN)_6$ suggests a centrosymmetric environment and k_5 is also small in this system,[60] as it is in some crystals containing $Cr(D_2O)_6^{3+}$.[60,118] In a trigonal complex, e.g., $Cr(ox)_3^{3-}$, the transition is electric dipole[27,119] and k_5 is markedly enhanced.

In addition to the estimation of k_5 from eqs 3 and 4, an upper limit for the radiative rate can be obtained from lifetime measurements by

$$\tau^{-1} = k_5 + k_6 \quad (5)$$

The very small value of k_6 in ruby, as demonstrated by the classic work of Nelson and Sturge,[25] leads to a close concordance between k_5 obtained from absorption and τ^{-1}. In contrast, k_5 is threefold larger than τ^{-1} in $Cr(CN)_6^{3-}$:$K_3Co(CN)_6$, a physically unacceptable result. Overlapping $^2T_1 \leftarrow {}^4A_2$ and $^2E \leftarrow {}^4A_2$ transitions might contribute to this discrepancy, but errors in evaluating f are more likely the problem. The results for the other crystalline systems are consistent with nonnegligible k_6 values.

The good agreement between k_5 and τ^{-1} for the four deuterated CrN_6 complexes in Table VI indicates that the decay in these systems is mainly radiative. In all cases, Φ_p/τ is markedly smaller than the k_5 value estimated from absorption spectra. These discrepancies could be explained by $\eta_D < 1$ but there is some overestimation of k_5 due to the use of room temperature $^2E \leftarrow {}^4A_2$ absorption coefficients. Systematic errors in the determination of Φ_p, especially in low-temperature glasses, cannot be excluded. That the Φ_p/τ values at low temperatures are 2–3 times larger than the corresponding quantities evaluated at room temperature, contrary to expectation, points to errors in the low-temperature Φ_p.

The k_5 trend with the halogen ligand in $Cr(NH_3)_5X^{2+}$ complexes suggests that ligand spin–orbit coupling is

not a significant factor in the radiative decay. Transfer of $Cr(CN)_6^{3-}$ from a centrosymmetric crystalline host to a glassy matrix increases the radiative rate to match the magnitude in the tetragonal complexes $Cr(NH_3)_5Cl^{2+}$ and $Cr(NH_3)_5Br^{2+}$.

Since k_5 is a population weighted average of the radiative rates from the ^2E components, thermal changes in k_5 can be due to population changes as well as to variations in the oscillator strengths. The oscillator strength for the lower energy R line in ruby is about 50% larger than for the higher energy component and the 10% lifetime increase between 20 and 195 K is due mainly to population changes.[25] There is very little information on the temperature dependence of k_5 for molecular complexes. An upper limit to the thermal enhancement of k_5 can be estimated from the temperature variation of τ^{-1}. This approach is limited to those complexes where k_6 is small at all temperatures. The $Cr(CN)_6^{3-}$:$K_3Co(CN)_6$ lifetime decrease from 125 to 50 ms between 77 and 300 K could be due to the change in k_5.[60] The low-temperature decay rates for 11 perdeuterated CrN_6^{3+} complexes are included in Table I. Seven of these have decay rates between 180 and 310 s^{-1}, close to the radiative rate, that are not dependent on the number of N–H bonds. τ^{-1} is exceptionally large in $Cr(D\text{-diamsar})^{3+}$ and $Cr(D\text{-dtne})^{3+}$, possibly due to an appreciable k_6. There is a hint of increased k_5 in *cis*-$Cr(D\text{-cyclam})(ND_3)_2^{3+}$.

The decrease in τ between 77 and 225 K is <15% in *trans*-$Cr(D\text{-cyclam})(ND_3)_2^{3+}$.[120] There is a τ *decrease* in the cis isomer of this species as the temperature is reduced below 100 K, while no corresponding change prevails for the trans isomer. The skeletal distortion is larger in the cis complex and τ decrease at low temperatures is consistent with different radiative decay rates from the ^2E components, coupled with population changes.

C. Nonradiative Rates

1. Theory

Radiationless transitions have been the subject of extensive theoretical attention.[8-10] While it is not possible to calculate absolute rates for polyatomic molecules, the theoretical models provide a framework for systematizing the corpus of experimental results and for determining the manner in which intramolecular and environmental changes affect relaxation rates. The theoretical approaches differ in detail but most contain several common features. Siebrand has presented a lucid summary of the basic ideas underlying the most widely used theory.[121] The point of departure is the Born–Oppenheimer approximation in which each state is represented by a product wave function

$$\Psi_{ai}(q,Q) = \Phi_a(q,Q)\Lambda_i^a(Q) \quad (6)$$

where $\Lambda_i^a = \prod_l \chi_{v_l}(Q_l)$. q and Q represent the electronic and nuclear coordinates, respectively, and v_l is the number of quanta in the lth vibrational mode. The Born–Oppenheimer approximation endows meaning to the multidimensional potential surface. The nonradiative transition from a → b is then "allowed" by mixing the zero-order Born–Oppenheimer functions under some interaction, usually vibronic. The basic rate equation then follows from the "golden rule"[11]

$$k_{nr}(a \rightarrow b) = \frac{2\pi}{\hbar}\sum_i\sum_j P(ai)|V_{ai,bj}|^2\delta(E_{ai} - E_{bj}) \quad (7)$$

where $P(ai)$ is the Boltzmann weight of a vibronic level in the initial electronic state. $V_{ai,bj} = \langle\Psi_{ai}|H'|\Psi_{bj}\rangle$ describes the mixing of the initial and final states under the interaction operator, H'. $\delta(E_{ai} - E_{bj})$ ensures that all the states in the summation satisfy the energy conservation requirement. In some formulations the δ function is replaced by ρ, the density of states in b.[121,122] Although spin–orbit coupling is involved in spin-forbidden transitions,[123] vibronic mixing is the key factor in mediating the radiationless transition. The modes responsible for the vibronic mixing are designated as promoting.[123a] At low temperatures in condensed media, only the lowest vibrational level in a is populated and if there is only a single promoting mode

$$k_{nr} = \beta F \quad (8)$$

where $F = \langle\Lambda^b|\Lambda^a\rangle$ includes the summation over all permutations of χ_{v_l} occupation numbers consistent with the energy conservation requirement. The promoting mode is omitted from Λ in evaluating F. The modes that contribute to F are called accepting. A harmonic mode can be accepting if there is a difference in equilibrium geometry along the relevant coordinate or a vibrational frequency change between the initial and final electronic states. In addition, anharmonicity can make a vibration accepting. β is the electronic factor and F the vibrational factor. If more than one promoting mode is important, k_{nr} is summed over the promoting modes

$$k_{nr} = \sum_k \beta_k F_k \quad (9)$$

In order to make the evaluation of eq 8 possible, assumptions are made and the several theoretical approaches are distinguished by these assumptions. Most of the attention has been focused on the computation of the Franck–Condon factors, F. The simplest model for this purpose is the displaced but undistorted harmonic mode approximation in which the coordinates of the accepting mode minima (Q_l) differ in the two states, the frequencies are unaffected by excitation, and only a single promoting and a single accepting mode are involved. In this case, the coupling strength is denoted by the Huang–Rhys factor, $S = (m_l\omega_l/2\hbar)(Q_l^{(a)} - Q_l^{(b)})^2$, a dimensionless measure of the horizontal displacement. Two limits are distinguished accourding to the magnitude of S.[11] In the weak-coupling limit, $S \ll 1$ and

$$k_{nr} = \beta \exp(-S) \exp(-\gamma(\Delta E/\hbar\omega_l)) \quad (10)$$

$$\gamma = \ln(\Delta E/S\hbar\omega_l) - 1$$

where ΔE is the difference in the energy of electronic origins in a and b, corrected for the energy of the promoting mode.

Equation 10 embodies the energy gap law wherein the nonradiative decay rate is an exponential function of the energy that must be transferred into the accepting modes. In this model, Q_l is the highest frequency accepting mode, and the variation of k_{nr} with the triplet → singlet transition energy in aromatics, where vibrations with large C–H stretching contributions are accepting, is in rough accord with this simple picture.[124] The reduction in ω_l by deuteration results in a marked decrease in the nonradiative decay rate since more quanta must be transferred into the C–D modes with

the consequent reduction of F. The dependence on the energy gap embodied in eq 10 is valid when more than three quanta of the accepting mode are excited,[125] a condition fulfilled in all of the transitions encountered in Cr(III) complex emission.

Robbins and Thomson were the first to attack the problem of the relationship between the structure of Cr(III) complexes and the $^2E \rightarrow {}^4A_2$ nonradiative rates.[12] Their analysis was based on the formalism of Englman and Jortner[11] and they assumed that the total horizontal displacement is $S = \sum_{i=1}^{n} S_i$, where n is the number of hydrogen atoms in the complex. Equation 10 then leads to

$$F = \text{const } (n)^{\Delta E/\hbar\omega_l} \quad (11)$$

They suggested on the basis of a limited data set that k_6 is a linear function of n and used a symmetry argument to conclude that the promoting vibrations are internal ligand modes. Since the increase in k_6 with n is much smaller than predicted by eq 11, which is based on the assumption that the variation is largely due to changes in the accepting-mode contribution, they emphasized the role of promoting modes in the nonradiative decay. Strek and Ballhausen,[126] expanding on the Robbins and Thomson theme that the major determinant of the variation in the nonradiative rate with the ligands is the change in the promoting-mode contributions to the electronic factor, used a modified approach in which the basis functions are products of functions that are localized in the CrL_6 skeleton and the intraligand modes. In this approach, the total rate is again expressed in terms of products of electronic and vibrational factors. A displaced undistorted coordinate model is assumed and the vibrational factor is computed in the usual way. The absence of skeletal modes of appropriate symmetry in octahedral complexes means that the intraligand modes are promoting. The application of this model to complexes of lower symmetry was made by Strek.[127]

Starting from eq 9, Kupka[128] evaluated F in a different way than did Englman and Jortner and included the effect of frequency changes in the accepting modes. He found that the influence of frequency changes is inversely related to the magnitude of the horizontal displacement. Since the displacement is very small in the $^2E \rightarrow {}^4A_2$ transition, the effect of the frequency changes could be dominant in Cr(III) complexes. Kupka found that a 10% reduction in ω_l leads to a k_6 enhancement of 10^{15} when $S = 0.25$. It must, however, be recognized that the frequency changes in the ligand-localized accepting modes will also be small.

Symmetry arguments enter the theoretical picture in several ways. For spin-forbidden transitions, β involves both vibronic and spin–orbit coupling. Since the spin–orbit interaction mixes wave functions that are localized on the metal ion, it is the skeletal symmetry that is pertinent for this contribution. The appropriate symmetry to be employed for the vibronic mixing depends upon the nature of the promoting mode. If this mode is skeletal, then the same symmetry is employed for both the spin–orbit and vibronic contributions to the electronic factor. If, on the other hand, ligand vibrations are promoting, the full molecular symmetry must be invoked. This symmetry, in turn, will depend upon the presence of rotational barriers for ligands such as NH_3 and H_2O. Only totally symmetrical vibrations contribute to S in the displaced undistorted coordinate model. Although reducing the symmetry, e.g., from O_h to D_3, would increase the number of accepting vibrations, the effect on S might be small. Furthermore, frequency changes and anharmonicity would tend to mask the effects of symmetry. In glassy media, where rotation about the metal–ligand bonds is inhibited, the molecular symmetry is so low that symmetry arguments lose their force for ligand-localized accepting modes.

The energy conservation constraint dictates that vibrations other than the promoting and accepting modes must be excited during the nonradiative transition. These "matching modes" are low-frequency intramolecular vibrations or solvent modes. It is generally assumed that their contribution to the decay is constant from one molecule to the next, at least in a closely related series.

The $^2E \rightarrow {}^4A_2$ transition in Cr(III) complexes is singular in two respects: (i) except for ligands that delocalize d electrons, there is little change in the transition energy with ligands; and (ii) the displacement of the potential energy minima is very small. Since large changes in the energy gap tend to obscure the influence of other molecular parameters, the near constancy of the transition energy permits examination of other factors.

In summary, theory suggests that the following questions be addressed in correlating k_6 and molecular structure: (1) the nature of the accepting and promoting modes, (2) the relative importance of energy gap and frequency changes, (3) the effect of anharmonicity, and (4) the role of geometry.

2. Low-Temperature Doublet-State Decay

Homoliganded Complexes. When ^2E is below $^4T_2$ the lifetime reaches a limit as the temperature is lowered where only minor lifetime changes occur upon further temperature reduction. This temperature is reached at 77 K for the complexes listed in Table I where the coordination is through the amine nitrogens in all six positions. These complexes are classified as homoliganded, even when the amine coordination involves different ligands as in *trans*-$Cr(cyclam)(NH_3)_2^{3+}$. The limiting lifetimes are insensitive to the composition of the glassy solvent when $k_5 \ll k_6$ unless there is a change in the character of the emitting state in different solvents, a situation not encountered in the homoliganded species.

The utility of the weak-coupling model for describing the effect of molecular structure on nonradiative rates is demonstrated by this large class of complexes. For a single dominant promoting mode, k_6 is a product of an electronic and a vibrational factor. F is inversely dependent on $\Delta E/\hbar\omega_l$, and the reduction of ω_l from 3200 cm^{-1}, the N–H frequency, to 2400 cm^{-1}, the frequency of the N–D vibrations, is accompanied by a drastic decrease in k_6. Although the τ^{-1} values for the deuterated complexes in Table VI are so close to the radiative lifetimes that reliable values of k_6 cannot be computed, the nonradiative rates are, with the exceptions of $Cr(D\text{-diamsar})^{3+}$, $Cr(D\text{-dtne})^{3+}$, and possibly *cis*-$Cr(D\text{-cyclam})(ND_3)_2^{3+}$, <100–200 s^{-1} in the perdeuterated CrN_6^{3+} complexes.

In the protiated amine complexes, $k_5 \ll k_6$ and τ^{-1} is a good measure of the nonradiative rate. In contrast

to the situation for k_5 in the deuterated complexes, the magnitude of k_6 increases with the number of N–H bonds. However, this dependence is much smaller than predicted by eq 1. The small S in the $^2E \rightarrow {}^4A_2$ transition would lead to a marked dependence of k_6 on ω_l differences in the ground and excited states. Kuhn et al. were able to fit the decay rate data to Kupka's model.[129] However, the fitting yielded 3–4% differences in ω_l upon excitation, and the N–H stretching frequency change is <1 cm^{-1}.[26]

Other factors that can affect k_6 are the energy gap and geometrical distortions. The energy gap for the $^2E \rightarrow {}^4A_2$ transition is fairly constant in the Cr(III) amines; with only one exception, the entire range in the transition energy is 14 600–15 200 cm^{-1}. The largest group of CrN_6^{3+} complexes contains 12 N–H bonds that are directly coordinated to the metal ion. Within this group the change in the energy gap is only 200 cm^{-1} and the small (15%) variation in k_6 appears to be correlated with the energy gap.[84] More pronounced changes in k_6 are associated with large conformational distortions. For example, the decay rate in $Cr(diamsar)^{3+}$ is threefold larger than in $Cr(tacn)_2^{3+}$, yet both complexes have 6 N–H bonds. The skeletal symmetry in $Cr(diamsar)^{3+}$ is considerably distorted from O_h.[130] $Cr(diamsar)^{3+}$ is exceptional in other respects; the decay rate reduction caused by deuteration is very small and the thermal quenching of the emission is unusual.[130,131] The deuterium isotope effect is also small in $Cr(dtne)^{3+}$, a complex that involves two tridentate ligands bridged by an ethyl group.[132] The skeletal distortion in $Cr(dtne)^{3+}$ is substantial,[133] and the decay rates in both the protiated and deuterated forms of this complex are exceptionally large for a species with only 4 N–H bonds. These results suggest that distortion enhances the nonradiative decay. A less pronounced, but nonetheless significant, conformational dependence is found in the isomers of $Cr(cyclam)(NH_3)_2^{3+}$, where the energy gap is not changed upon isomerization. The emission spectra of the trans complex[100] and $Cr(NH_3)_6^{3+}$ are similar; the 0–0 bands are relatively weak in both. The emission spectrum of the cis complex resembles that of $Cr(en)_3^{3+}$, where the skeletal distortion is substantial. The decay in the cis isomer is distinctly faster than in the trans analogue.

At issue is the source of the geometry dependence. The deuterium isotope effect clearly establishes the intraligand N–H vibrations as the dominant accepting modes. Only totally symmetric modes are accepting in the displaced-coordinate approximation. It has been suggested that the small k_6 enhancement associated with five-membered rings is due to the increase in the number of totally symmetric modes accompanying the reduction in symmetry.[129] However, when the decay rates for complexes are plotted against the energy gap, the data for five-membered rings do not exhibit exceptional behavior.[84] Instead, the distortion diminishes the energy gap slightly with a concomitant increase in k_6. Skeletal symmetry is a poor indicator of the appropriate symmetry to be used to classify the intraligand modes since the environmental distortions induced by the rigid glass lower the global molecular symmetry.

Although the overall molecular symmetry has little effect on the ligand-localized accepting modes, the efficacy of a skeletal promoting mode may depend on the geometry. For example, the k_6 enhancement attendent upon the conformational distortion in *cis*-$Cr(cyclam)(NH_3)_2^{3+}$ could be due to the increase in the electronic factor induced by the symmetry reduction in the cis isomer.

The $^2E \rightarrow {}^4A_2$ nonradiative decay rates for other homoliganded species are collected in Table II. In the CrN_6^{3+} complexes there is hardly any lifetime increase below 77 K. However, when the ^2E–$^4T_2$ separation is small, a different situation is encountered, as exemplified by $Cr(D_2O)_6^{3+}$. In glassy media, the limiting lifetime is reached a little below 77 K for this complex, but in dilute chrome alum, no limit is observed down to 4 K.[134] The ^2E–$^4T_2$ separations are also small in the thiocarbamate complexes, but the published lifetime data are insufficient to decide if the low-temperature limits were reached at 77 K. The decay rates for the remaining complexes in Table II are the low-temperature limits.

The quenching propensity of ligands in homoliganded complexes can be designated as high, moderate, and low.[135] Good quenchers are arbitrarily characterized by $k_6 > 4000\ s^{-1}$ and $\tau^{-1} \approx k_6$ in this case. Protiated amines, DMSO, and H_2O belong to this group. At the other extreme are the poor quenchers phen, bpy, NCS^-, D_2O, CN^-, and the perdeuterated amines. The lifetimes in homoliganded complexes with these ligands are very close to radiative. acac and ox are examples of moderate quenchers. With the exception of DMSO, the good quenchers contain N–H and O–H bonds directly coordinated to the Cr^{3+} ion. The vibrational energies of these bonds are large, >3200 cm^{-1}, and are good accepting modes. On the contrary, the highest energy vibrations in CN^- and NCS^- are small, <2200 cm^{-1}. There are high-energy C–H vibrations in the diimines phen and bpy, yet the k_6 are very small in complexes with these ligands. However, the C–H bonds are on the periphery of these ligands. A vibration will not be a good acceptor unless the d-electron density is appreciable in the vicinity of the bond in question.[12] The small nephelauxetic effect in the diimine complexes indicates little d-electron delocalization onto the ligands, and consequently the C–H modes do not contribute significantly to k_6. This interpretation is supported by the fact that acac is a moderate quencher. In this ligand the C–H bonds are also distant from the metal ion but the d-electron delocalization, as measured by the nephelauxetic effect, is very large. k_6 increases as large as tenfold are attendent upon replacement of the methyl groups in acac by hydrogen atoms or phenyl groups and are correlated with a concomitant increase in d-electron delocalization.[5] No high-frequency modes in ox, urea, and DMSO are effectively coupled to the metal ion, and neither the relatively large k_6 in $Cr(DMSO)_6^{3-}$ and $Cr(urea)_6^{3+}$ nor the moderate value in $Cr(ox)_3^{3-}$ is readily explained by delocalization.

Heteroliganded Complexes. The results for CrA_nB_{6-n} complexes (n = 1–5) are collected in Tables III and IV. There are only eight A–B pairs in which the data are extensive, viz., NH_3–H_2O, NH_3–D_2O, ND_3–D_2O, NH_3–NCS^-, H_2O–CN^-, en–ox, D-en–ox, and DMSO–NCS^-. When trying to relate k_6 to n in a CrA_nB_{6-n} series, one must recognize that the energy gap can vary with n. This is especially important when ligands with large nephelauxetic effects are involved, e.g., CN^- and

NCS^-. In addition, the possibility of level inversion between ^2E and $^2E^Q$ must be kept in mind when large tetragonal splittings obtain.[82,86] Robbins and Thomson posited additive ligand contributions to the k_6 for CrA_nB_{6-n} complexes in which O–H and N–H vibrations were the main accepting modes.[12] They attributed the correlation of k_6 with the number of H atoms to variations in the promoting-mode efficiencies with n. This suggestion was based on a small data set and the simple additive independent-ligand model. This model, where $k_6 = nk_A + (6 - n)k_B$, is not supported by the data in Tables I–IV. In a modified independent-ligand model, $k_6 = k_A + k_B$, and the contributions of the A and B ligands were separately calculated by Kupka's method.[136] Thus, in $Cr(NH_3)_4(H_2O)_2^{3+}$ 12 N–H accepting modes were assumed in the calculation of k_{NH_3}, while k_{H_2O} was estimated for 4 O–H vibrations. The electronic factors appropriate to the corresponding homoliganded species were used unchanged. The validity of this approach was supported by the apparent good agreement between the calculated and experimental k_6 in several partially deuterated NH_3–H_2O complexes.[137] However, there was a discrepancy between these experimental k_6 values and those reported previously.[138] The earlier $Cr(NH_3)_5(D_2O)^{3+}$ value has now been confirmed.[139] No independent-ligand model has yet been validated.

Since ligand substitution can affect ΔE as well as the promoting and accepting modes, both the electronic and vibrational factors can change and no simple relationship between k_6 and n is to be expected. The rate enhancement that accompanies replacement of ligands with good accepting modes by monatomic ligands also highlights the danger of focusing on the accepting modes when trying to explain ligand substitution effects. Several significant trends emerge from examination of Table III. In three sequences, replacement of N–H by F^- is correlated with a marked k_6 increase. Although Cl^- is somewhat more effective than F^- in k_6 enhancement, some of the difference is associated with a decreased energy gap. The effect of F^- is much smaller in the highly distorted *cis*-cyclam complex. As in the case of radiative rates, increased spin–orbit coupling induced by halide ligation is not an important factor for the nonradiative rates.

Changes in skeletal symmetry occasioned by isomerization have little effect on k_6 in glassy solutions of $Cr(NH_3)_4X_2$ and $Cr(en)_2X_2$ complexes. However, when diluted into crystalline hosts, the decay rate in *cis*-$Cr(en)_2Cl_2^+$ is twice that of the trans counterpart. The importance of conformational distortion is underscored by the results for the diaquo complexes with cyclam ligands. Not only is k_6 larger in *cis*-$Cr(cyclam)(H_2O)_2^{3+}$ than in the trans analogue, but the increased distortion induced by the cyc*b* ligand is also evident.

In $Cr(NH_3)_{6-n}(NCS)_n^{3-n}$, $Cr(H_2O)_{6-n}(CN)_n^{3-n}$, and $Cr(DMSO)_{6-n}(NCS)_n^{3-n}$ complexes there is a monotonic decrease in k_6 as a good or moderate quenching ligand is replaced by a poor quencher. Correction for the progressive decrease in the energy gap with n would only serve to accentuate this trend. In contrast, the $Cr(NH_3)_{6-n}(D_2O)_n^{3+}$ and $Cr(en)_{3-n}(ox)_n^{3-2n}$ complexes exhibit maxima in the k_6 versus n dependence. Within the simple model embodied in eq 8 this would indicate that the electronic factors are increased by oxygen coordination, while the vibrational factor decreases with n. The monotonic increase in τ^{-1} with n in the $Cr(D\text{-}en)_{3-n}(ox)_n^{3-2n}$ series is consistent with this supposition.

In the foregoing, it was assumed that the emission was $^2E \rightarrow {}^4A_2$. In the CrN_4X_2 isomer pairs, where the emission of the trans complex is $^2E^Q \rightarrow {}^4A_2$ and the cis complex emission is $^2E \rightarrow {}^4A_2$, the assessment of the isomer effect is more uncertain since estimation of the energy gap in the broad spectrum of the trans complex is difficult. Since the ^2E energy is essentially the same in both isomers, observation of the broad-band emission demonstrates that $^2E^Q$ is below ^2E. The smaller energy gap would lead to a larger k_6 in the trans isomer. In addition, the larger horizontal displacement in $^2E^Q$ would enhance k_6. In the $Cr(NH_3)_4(OH)_2^+$, $Cr(en)_2(OH)_2^+$, and $Cr(en)_2F_2^+$ pairs, k_6 is larger in the trans complex. However, $Cr(NH_3)_4F_2^+$ does not fit into this picture because the decay is faster in the cis isomer.

The $^2E^Q$ energy is solvent dependent and k_6 does increase as the $^2E^Q$ energy is lowered.[86,87]

Environmental Effects on Excited-State Decay Rates. Several sources for the variation in the low-temperature limiting lifetime with host can be imagined. Decay rates in pure crystals are sensitive to intermolecular interactions and solid-state defects. For example, the ^2E lifetime of $Cr(ox)_3^{3-}$ ranges from 960 μs in $NaMgCr(ox)_3 \cdot 9H_2O$[104] to 180 μs in $K_3Cr(ox)_3 \cdot 3H_2O$.[106] Comparable lattice effects prevail for $Cr(en)_3^{3+}$, $Cr(urea)_6^{3+}$, and $Cr(acac)_3$.[16] None of the results collected in Tables I–IV refer to pure crystals.

In dilute crystals and glasses, differences in site symmetry and environmentally induced distortions can affect the decay rate. There are a number of complexes for which the limiting lifetimes have been recorded in glasses and in a dilute crystal (Tables I–III). The lifetimes of $Cr(acac)_3$, $Cr(ox)_3^{3-}$, $Cr(NH_3)_6^{3+}$, and *trans*-$Cr(en)_2Cl_2^+$ are nearly the same in the two media. On the other hand, the ^2E decay in *cis*-$Cr(en)_2Cl_2^+$ is 50% faster in a dilute crystal. A most striking environmental effect is seen in $Cr(CN)_6^{3-}$, where the decay rate is enhanced 35-fold when the host is changed from crystalline to glassy. $Cr(D_2O)_6^{3+}$ is of especial interest. In this species $^4T_2$ and ^2E are nearly equienergetic and the lifetime is very sensitive to the nature of the crystalline host.[16]

A number of noncrystalline "frozen" solvents have been employed. In some cases, quick freezing of a pure solvent will produce a transparent, albeit cracked, glass. More usually, a microcrystalline opaque mass will be formed. The rate of cooling can be important. For example, if DMF is cooled by direct immersion into liquid N_2, microcrystals result unless the diameter of the sample tube is 1–2 mm. A glass will be formed in the narrow tube because the rate of cooling is fast. The preponderence of the published low-temperature photophysical data refer to mixed solvents, either alcohol–water or DMSO–water. In a few cases, pure DMSO was used, but no details about the nature of the frozen solutions were given.[140]

It is important to distinguish possible solvent effects on k_5 and k_6 since k_5 is sensitive to skeletal symmetry while k_6 is not. The ^2E lifetime is nearly the same for amine complexes in glassy alcohol–water, DMSO–water, DMF–water, and frozen microcrystalline DMSO.[140] However, there is a twofold variation in the $Cr(NCS)_6^{3-}$ lifetime when the solvent is changed from alcohol–water

to frozen DMSO.[87] The decay in $Cr(NCS)_6^{3-}$ is nearly radiative and these data suggest that k_5 is much more dependent on solvent than is k_6. Additional support for this view comes from the results for the Cr(cyclam)$(NH_3)_2^{3+}$ isomers.[120] The low-temperature lifetimes of both the cis and trans protiated isomers, where $k_6 \gg k_5$, vary with solvent by <15% in alcohol–water, DMSO–water, and DMF. However, in the deuterated analogues ($k_6 \ll k_5$), there is a substantial lifetime difference between the DMSO–D_2O and DMF glasses, approaching 100% in the trans species.

The possibility of a solvent effect on k_6 cannot be excluded. When intramolecular contributions to k_6 are small, solvent vibrations may be accepting. Some of the lifetime variation in $Cr(NCS)_6^{3-}$ and *trans*-Cr(D-cyclam)$(ND_3)_2^{3+}$ may be due to the solvent dependence of k_6.

When the $^4T_2$–^2E gap is small enough to permit some back-transfer at 77 K, e.g., $Cr(D_2O)_6^{3+}$ and $Cr(urea)_6^{3+}$, the decay in a glassy solvent becomes nonexponential. This is due to the site to site variation in k_{-4}.

Another example in which a distribution of sites plays a role is $Cr(CN)_6^{3-}$ in a rigid glass where $k_6 \gg k_5$.[141] The decay is exponential when the excitation wavelength is 366 nm or less. However, excitation into the red edge of the $^4T_2 \leftarrow {}^4A_2$ band leads to nonexponential decay. In addition, the emission spectrum varies with excitation wavelength. Surprisingly, this effect apparently persists in a fluid medium,[142] although impurity emission cannot be ruled out at ambient temperatures. The great sensitivity of the $Cr(CN)_6^{3-}$ emission to a change in the environment from dilute crystal to glass has been described above. Further evidence for a solvent effect on this complex is the nearly fourfold decrease in decay rate occasioned by changing from an alcohol–H_2O to a DMF glass.[143]

The ^2E energy is essentially independent of environment, but in quadrate complexes $^2E^Q$ varies with solvent.[86,87] When the emission is $^2E^Q \rightarrow {}^4A_2$ solvent-induced changes in the energy gap will affect k_6. Even more striking is the change in decay rate that accompanies ^2E–$^2E^Q$ level inversion. The decrease in the 77 K lifetime of *cis*-Cr(phen)$_2F_2^+$ from 1400 μs in alcohol–water to 800 μs in a DMF glass is an example of this phenomenon.

Solvent effects associated with solvent mobility constitute a different class of environmental perturbations that will be discussed in section IV.C.5.

3. $^4T_2 \rightarrow {}^4A_2$ Decay Kinetics

When ^2E is below $^4T_2$ a temperature can be achieved where k_{-4} is negligible, and $k_5 + k_6$ can then be directly determined from the lifetime. Since $^4T_2$ is rarely the lowest excited state in molecular complexes, $k_2 + k_3$ cannot often be extracted directly from lifetime measurements. Except for complexes with sulfinate coordination, the fluorescence in molecular complexes is delayed, i.e., follows back-transfer from ^2E. In these cases, λ_1 contains contributions from k^T but the estimation of $k_2 + k_3$ is not unambiguous.

Although thermally activated $^4T_2 \rightarrow {}^4A_2$ emission is observed in $Cr(urea)_6^{3+}$ and related complexes,[52,58] delayed fluorescence in $Cr(D_2O)_6^{3+}$ is very weak,[60] suggesting that $k_3 \gg k_2$ even at low temperatures in this latter species. According to eqs 1 and 2, the decay rate should be λ_1 for both delayed fluorescence and phosphorescence. The decays from glassy solutions of $Cr(urea)_6^{3+}$ and $Cr(atp)_6^{3+}$ were nonexponential, and the decay rates differed for emission monitored in the fluorescence and phosphorescence emission regions.[58,59] That this behavior is due to different sites in which there is a distribution of decay rates is shown by the results in $[Cr(urea)_6](ClO_4)_3$ and $[Cr(urea)_6]I_3$, where the decays were exponential and independent of monitoring wavelength.[60] In these two crystals, a unique environment exists.

Small changes in ligand structure can affect k_3 profoundly. This is demonstrated by the total absence of delayed fluorescence in $Cr(imid)_6^{3+}$.[144] The only difference between imid and urea is the presence of an ethylene bridge between the NH_2 group in the former ligand.

There are a number of ionic crystals and glasses containing Cr^{3+} in which $^4T_2$ is below ^2E.[67] The oscillator strengths for $^4T_2 \leftarrow {}^4A_2$ lie in the 10^{-4}–10^{-5} range and the corresponding k_2 values are 10^3–10^4 s^{-1}. $CrCl_6^{3-}$ in Cs_2NaYCl_6 is accurately O_h; the $^4T_2 \leftarrow {}^4A_2$ origin is due to a magnetic dipole transition even though $^4T_2$ suffers a Jahn–Teller distortion.[23] k_2 as calculated from the oscillator strength is 2.5×10^3 s^{-1},[22] while $\tau^{-1} = k_2 + k_3 = 6.7 \times 10^3$ s^{-1}.[145] The low-temperature limit for the lifetime is not reached at 4 K for this complex in $Cs_2NaScCl_6$ and 6×10^3 s^{-1} is a lower limit for the decay rate.[146] The $^4T_2$ decay rate for CrF_6^3 in ionic crystals is 2×10^3 s^{-1}.[22] The emission quantum yield is high in these systems, approaching unity in a K_2NaScF_6 host.[147] Consequently, k_3 is very small, as expected from the theory since the accepting modes are the low-frequency skeletal vibrations.[148]

The emission spectra from inorganic glasses containing Cr(III) are often broad and at a position consistent with the $^4T_2 \rightarrow {}^4A_2$ transition. The decays are nonexponential, indicating a distribution of emitting species.[68] When Cr^{3+} is doped into $Al(PO_3)_3$, a CrO_6 "complex" is presumed to exist, and both crystalline and glassy phases have been prepared.[149] The decay rate is 6×10^3 s^{-1} in the centrosymmetric crystalline sites but tenfold larger in the glass. Andrews et al. argued that the enhancement in the glass is due to an increase in k_3 which results from a reduction in site symmetry. However, lowered symmetry would also increase k_2. The $^4T_2 \leftarrow {}^4A_2$ oscillator strength for $Cr(H_2O)_6^{3+}$ in $K_2Cr(SO_4)_3 \cdot 12H_2O$, where the environment is markedly trigonally distorted, is 1.6×10^{-4}.[150] An extreme example of k_2 enhancement is encountered in the highly distorted trigonal sites of Cr^{3+}:$LiNbO_3$. The contribution of $^2E \rightarrow {}^4A_2$ emission is negligible at 4 K and the decay rate of the broad emission is 10^5 s^{-1}.[151] The emission yield in this system is nearly unity and the decay is essentially radiative.

A 50-ps emission has been observed at 500–650 nm for a number of Cr(III) complexes under intense 335-nm excitation.[152] This emission, which is absent under 532-nm excitation, has been ascribed to emission from unrelaxed $^4T_2$ and has no relevance to the estimation of k_3 that pertains to decay from thermalized $^4T_2$. Rojas and Magde report a weak broad band in room temperature aqueous solutions of *trans*-$Cr(NH_3)_2(NCS)_4^-$ and $Cr(NCS)_6^{3-}$.[51] These emissions overlap the narrower phosphorescence but exhibit a different temporal

behavior and were assigned as prompt fluorescence. If this assignment is correct, k_3 exceeds 10^{10} s^{-1} under these conditions. Prompt fluorescence was also observed in solutions of $Cr(urea)_6^{3+}$ and $Cr(ox)_3^{3-}$.[153]

4. Intersystem Crossing Efficiencies and Rates

In eqs 1 and 2 two pathways for nonradiative transfer from $^4T_2$ to the doublet manifold have been distinguished, and it is assumed that prompt intersystem crossing produces $[^2E]_0$ on a time scale that is too fast to monitor; i.e., the population of ^2E by the prompt process is indistinguishable from that induced by direct $^2E \leftarrow {}^4A_2$ absorption. However, if either the prompt crossing rate or k_4 is small on the measurement time scale, a rise time in the $^2E \rightarrow {}^4A_2$ emission will be observed. No rise time was detectable in the emission of $Cr(en)_3^{3+}$, $Cr(urea)_6^{3+}$, $Cr(ox)_3^{3-}$, $Cr(CN)_6^{3-}$, $Cr(acac)_3$, and ruby within the ≈1-ns resolution time of the instrument.[154] Transient absorption measurements with solutions of $Cr(NH3)_2(NCS)_4^-$, $Cr(NCS)_6^{3-}$, $Cr(acac)_3$, and $Cr(en)_2(NCS)_2^+$ yielded delays in the appearance of the transient absorption, thought to originate in ^2E, as large as 29 ps,[155,156] but repetition of these experiments with 1-ps resolution failed to reveal any delay in the appearance of the transient.[157] The slow rise time (10–20 ns) in the $Cr(phen)_3^{3+}$ and $Cr(bpy)_3^{3+}$ $^2E \rightarrow {}^4A_2$ emission[158] has been questioned.[159,160] It appears that ^2E is populated in <1 ns and that the slower transients are associated with multiphoton events induced at high laser power.[161]

It is difficult to excite the $v = 0$ level in $^4T_2$ by direct absorption, and the $^4T_2 \rightarrow {}^2E$ intersystem crossing rates were measured subsequent to excitation of higher vibrational levels in $^4T_2$. Consequently, it is possible that the very fast intersystem crossing is prompt and that k_4 is smaller than 10^{12} s^{-1}. ^2E is slightly above $^4T_2$ in Cr^{3+}:$LiTaO_3$, and the line width of the $^2E \leftarrow {}^4A_2$ 0–0 band at 4 K is 50 cm^{-1}.[151] This corresponds to a decay rate near 10^{13} s^{-1}, which can be identified with k_4. The evidence strongly favors a very fast intersystem crossing rate.

Although the intersystem crossing rates have not been directly measured, some information about intersystem crossing efficiencies is available. The most direct approach to determining the fraction of initially populated $^4T_2$ that reaches ^2E[162]

$$\eta_D = \eta_{pisc} + (1 - \eta_{pisc})\eta_{isc} \qquad (12)$$

is to compare the phosphorescence or photolysis quantum yields obtained by $^4T_2 \leftarrow {}^4A_2$ and $^2E \leftarrow {}^4A_2$ excitation. Equation 12 is not valid when k_{-4} is appreciable and η_D might be temperature dependent. The results described here refer to ambient temperatures. The ratio of the $Cr(en)_3^{3+}$ luminescence yield excited at 514.5 nm to that excited at 668.9 nm is 0.68.[162] The $^2E \leftarrow {}^4A_2$ transition is well resolved in the solution absorption spectrum of this complex, and 668.9-nm radiation is presumed to directly excite ^2E. The total photolysis yield upon 668.9-nm excitation is 0.45, compared to the 514.5-nm value, 0.42. Thus, within experimental error (15%), the photolysis yield is the same for quartet and doublet irradiation. The $Cr(en)_3^{3+}$ photochemistry consists of two components, one of which is not affected by quenching of the ^2E level. The quenchable photochemistry arises either from reaction in ^2E or from $^4T_2$ after population from ^2E and constitutes approximately 60% of the total photoreaction.[163] The ratio of the quenchable photolysis after $^4T_2$ excitation to the directly excited ^2E reaction, 0.64, is again η_D. However, in another study of $Cr(en)_3^{3+}$, the directly excited ^2E photolysis yield was 0.53–0.59 and the yield under $^4T_2$ excitation only 0.37,[164] leading to $\eta_D = 0.45$. In spite of the uncertainties in η_D, since the unquenchable photochemical yield is 0.11, nonradiative decay from $^4T_2$ to $^4A_2$ is significant. Although precise magnitudes for η_{isc} and η_{pisc} cannot be extracted from η_D in this case, some limits can be placed on these quantities. Using Kirk's data,[162] one finds that the maximum value for either η_{isc} or η_{pisc} is 0.66 ± 0.02. The variation of the emission quantum yield following excitation into various parts of the $^4T_2 \leftarrow {}^4A_2$ band has been examined with the aim of determining the dependence of intersystem crossing yield on the $^4T_2$ vibrational level initially populated. Evidence that η_D is smaller for excitation into the long-wavelength tail of the $Cr(en)_3^{3+}$ absorption band at 514 nm than for excitation at 436 nm has been presented.[165–168] However, in another study there was no wavelength dependence of the emission yield in the 374–530-nm range.[169] No resolution of this conflict is apparent. A wavelength-dependent emission yield has also been reported for *trans*-$Cr(en)_2(NCS)_2^+$.[170]

Estimates of η_D have been made by comparison of direct and sensitized emission.[171,172] In fluid media these studies led to the following values for η_D: 0.5 for $Cr(CN)_6^{3-}$ in DMF, 0.45 for $Cr(en)_2(NCS)_2^+$ in H_2O, 0.94 for $Cr(bpy)_3^{3+}$ in H_2O, and 0.71 for $Cr(en)_3^{3+}$ in H_2O. There is evidence that η_D is near unity when $Cr(CN)_6^{3-}$ and $Cr(en)_3^{3+}$ are dissolved in crystalline hosts.[173,174] The reduction of η_D in fluids can be explained by prompt $^4T_2$ photochemistry or nonradiative $^4T_2 \rightarrow {}^4A_2$ decay.

5. Temperature-Dependent Decay Processes

In contrast to the multitude of rates available for doublet-state decays at low temperatures, data on the temperature variation of these rates are limited. The effect of temperature in the 77–300 K interval ranges from very large to very small. Possible thermal decay processes for the depopulation of ^2E are (1) enhanced $^2E \rightarrow {}^4A_2$, (2) $^2E \rightarrow {}^4T_2$ back-transfer, and (3) chemical reaction.

The enhancement of the decay rate is represented by increases in k_5, k_6, and k_{-4} in eq 1. If chemical reaction competes kinetically with the other two pathways, λ_1 will be affected by ^2E photochemistry and be manifested by an increase in k_6. Two primary photolytic processes can be imagined in solution, dissociative and associative. These processes, as well as the distinction between direct ^2E and solvent-promoted surface crossing,[175] will be treated in section IV.D.

All three of the thermal decay processes can depend upon the environment, especially solvent viscosity. Environmental effects are clearly evident in the thermal enhancement of the $Cr(acac)_3$ excited-state decay. When $Cr(acac)_3$ was dissolved in a series of alcoholic solvents, the abrupt decreases in lifetime with temperature were attributed to decreases in solvent viscosity.[56] If the ^2E–$^4T_2$ separation is reduced by solvent motions, the rate of back-transfer would be increased.

Also, associative reactions with the solvent would be facilitated by solvent mobility on the excited-state time scale. Finally, solvent relaxation can increase the nonradiative rate by reducing the excited state–ground state energy gap.[120] Schläfer et al. found that the thermal quenching of emission from $Cr(CH_3NH_2)_5Cl^{2+}$, *cis*-$Cr(en)_2Cl_2^+$, *cis*-$Cr(en)_2Br_2^+$, $Cr(NCS)_6^{3-}$, and $Cr(CN)_6^{3-}$ in glassy solvents was related, in some cases, to the conversion of the rigid glass to a fluid.[176] That solvent rigidity need not be the dominating factor was demonstrated by Pfeil, who showed that the temperature for the onset of thermal quenching varied in the same alcohol–water solvent from 150 K for $Cr(acac)_3$ to 230 K for $Cr(en)_3^{3+}$.[177]

For the purpose of classifying ^2E thermal quenching phenomena, it is useful to categorize Cr(III) complexes according to the magnitude of the ^2E–$^4T_2$ energy gap. When this gap is large compared to the thermal energy, back-transfer is negligible. $Cr(CN)_6^{3-}$ is an example of this behavior. At the other extreme stand those complexes with a small gap that permits appreciable population of $^4T_2$ at 77 K. $Cr(urea)_6^{3+}$ belongs to this second class. In glassy solutions of $Cr(urea)_6^{3+}$ and the related $Cr(atp)_6^{3+}$ both fluorescence and phosphorescence are observed at 84 K and the fluorescence intensity increases relative to the phosphorescence intensity as the temperature is increased.[52] This clearly implicates back-transfer as a thermal decay pathway. However, the fluorescence and phosphorescence lifetimes are not the same as would be expected if all of the fluorescence were delayed.[59] In addition, the relative intensities of the two emissions are concentration dependent. The ^2E–$^4T_2$ gap is also small in $Cr(H_2O)_6^{3+}$, and thermally induced weak fluorescence is detectable when $Cr(D_2O)_6^{3+}$ is dissolved in a crystalline host.[60] The bulk of the Cr(III) complexes fall into an intermediate category, and it is these complexes that have been subject to considerable discussion.[18,153,178-184] If delayed fluorescence is detected, back-transfer is unambiguously identified. The weak broad luminescence bands in room temperature aqueous solutions of $Cr(ox)_3^{3-}$, *trans*-$Cr(NH_3)_2(NCS)_4^-$, and $Cr(NCS)_6^{3-}$ have been interpreted as delayed fluorescence.[153] The broad ambient temperature luminescence from solutions of amine complexes containing fluoride has also been assigned as fluorescence[89] but $^2E^Q \rightarrow {}^4A_2$ cannot be excluded.[87] The absence of delayed fluorescence does not rule out back-transfer since k_3 may be very large relative to k_2. In the early work, identification of back-transfer as a thermal decay process was based on the magnitude of the activation energy for thermal quenching.[60] If this activation energy corresponded to the ^2E–$^4T_2$ separation, back-transfer was presumed to be involved. Assessment of the energy gap is difficult because the 0–0 band of the $^4T_2 \rightarrow {}^4A_2$ transition is usually not resolved, although some criteria have been advanced for this estimation (section III.B). The change in the $^4T_2$ energy with solvent relaxation further complicates the picture.

In the limit of negligible k_{-4}, $\tau_0^{-1} = k_5 + k_6$ and

$$\tau^{-1} - \tau_0^{-1} = k_5 - (k_5)_0 + k_6 - (k_6)_0 \qquad (13)$$

Changes in k_5 are usually small and $k_6 - (k_6)_0$ contains contributions from thermally activated nonradiative decay and ^2E reaction. If both of these processes are important and each exhibits an Arrhenius dependence,[185] the thermal contribution to the decay is described by a two-term function

$$\tau^{-1} - \tau_0^{-1} = s_1 \exp(-E_1/RT) + s_2 \exp(-E_2/RT) \qquad (14)$$

The thermal dependence of the $Cr(acac)_3$ lifetime in alcohols was fitted to eq 14,[56] but Allsopp et al. suggested that a single-term Arrhenius dependence was adequate to fit the data for $Cr(acac)_3$ and several other complexes.[186] Unless the $^4T_2$–^2E separation is small, there is typically a substantial temperature region above 77 K where only a small τ decrease is observed. The radiative rates may change slightly with temperature in this range, largely due to variations in the population of the ^2E components,[25] but the small activation energies at low temperatures (<1 kcal mol^{-1}) are consistent with the involvement of a low-energy vibration in the thermally activated nonradiative $^2E \rightarrow {}^4A_2$ decay process.[185] The values of the Arrhenius parameters for the low-temperature process are very sensitive to the magnitude of the low-temperature-limiting lifetimes used in the fitting, and seldom will the data quality be good enough to extract a precise value for E_1. The analysis is complicated by abrupt changes in the lifetime that occur even when the solvent is quite rigid.[120] It is easier to test the applicability of an Arrhenius analysis in the high-temperature domain where the contribution of the low-temperature process to the overall decay rate is small.

When k_{-4} is significant, the ^2E decay rate is no longer $k_5 + k_6$ and eq 13 is not valid. In order to derive information about thermal changes in the individual rate constants from the overall ^2E decay rate, it is necessary to find a suitable approximation for $\lambda_1 = \tau^{-1}$. Two limits have been used to describe the exponential decay of ^2E.[15] If $4k_4k_{-4} \ll (k_T - k_E)^2$

$$\tau^{-1} = k_E - k_4k_{-4}/(k_T - k_E) \qquad (15)$$

At the other extreme is the "equilibrium" limit in which $k_4 \gg k_2 + k_3$ and $k_{-4} \gg k_5 + k_6$. This leads to

$$\tau^{-1} = [k_5 + k_6 + (k_2 + k_3)K]/(1 + K) \qquad (16)$$

where $K = k_{-4}/k_4$.

When $k_T \gg k_E$, eq 15 reduces to

$$\tau^{-1} = k_5 + k_6 + (1 - \eta_{isc})k_{-4} \qquad (17)$$

where $\eta_{isc} = k_4/(k_2 + k_3 + k_4)$.

Calculations show that eq 17 is a good approximation to λ_1 when $\eta_{isc} = 0.1$–0.99 for all reasonable values of $k_2 - k_6$ consistent with a lifetime decrease of 100-fold over the temperature range involved. Sometimes eq 15 or 16 fails badly under these conditions and neither is ever superior to eq 17. Subject to the assumptions that neither k_5 nor η_{isc} is temperature dependent

$$\tau^{-1} - (\tau^{-1})_0 = k_6 - (k_6)_0 + (1 - \eta_{isc})k_{-4} \qquad (18)$$

and $k_6 - (k_6)_0$ can be identified with the thermal dependence of the nonradiative decay and s_1 and E_1 in eq 14. If the high-temperature process is back-transfer, E_2 is the $^4T_2$–^2E energy gap and $s_2 = (1 - \eta_{isc})k_4$. If back-transfer is negligible, the small activation energy in a two-term Arrhenius fit to eq 14 would be associated with a low-frequency nonradiative contribution to k_6, while the higher energy activation energy could refer to ^2E reaction or to a second nonradiative process.

The putative concordance of E_2 with the $^4T_2$–^2E separation has been used to implicate back-transfer as a decay pathway at higher temperatures. According to

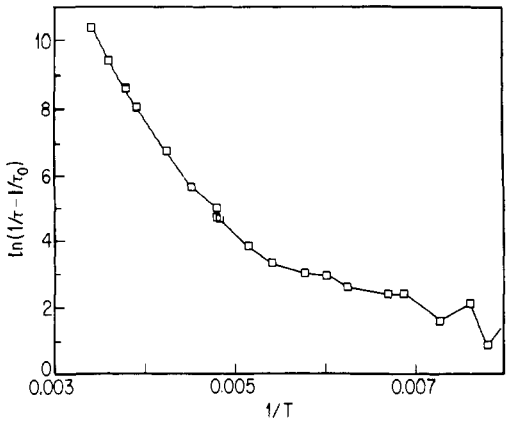

Figure 6. Temperature dependence of the $Cr(bpy)_3^{3+}$ excited-state decay, corrected for the low-temperature limiting rate, in ethylene glycol/H_2O (2:1 (v/v)).

this criterion, back-transfer is not a plausible decay pathway for CrN_6^{3+} complexes.[184,187] E_2 is 1200 cm^{-1} for $Cr(ox)_3^{3-}$ and 2600 cm^{-1} for $Cr(acac)_3$.[60] Fleischauer et al. give the $^4T_2$–^2E energy differences for these two species as 1370 and 3280 cm^{-1}, respectively.[55] On this basis, back-transfer is a feasible thermal decay process in $Cr(ox)_3^{3-}$. The observation of delayed fluorescence at room temperature in $Cr(ox)_3^{3-}$, $Cr(NCS)_6^{3+}$, and *trans*-$Cr(NH_3)_2(NCS)_4^-$ but not in *trans*-$Cr(en)_2(NCS)_2^+$, $Cr(en)_3^{3+}$, and *trans*-$Cr(py)_4F_2^+$ has led to the criterion that back-transfer is significant when the $^4T_2$–^2E gap is less than ≈3400 cm^{-1}.[153] The $^4T_2$ energy could be lowered relative to ^2E when the rigid glass melts, and application of the Schläfer rule would then lead to an overestimate of the gap in fluid media.

Although there are some quantitative differences in the one- and two-term fits to the $Cr(acac)_3$ data,[15,56] in both analyses the activation energy is reduced more than fivefold by chloride substitution in the 3-position on the acac ligand.

The ^2E–$^4T_2$ gap is small in $Cr(H_2O)_6^{3+}$ as evidenced by the observation of delayed $^4T_2 \rightarrow {}^4A_2$ emission in $Cr(D_2O)_6^{3+}$.[60] The more than fourfold difference in the 77 K lifetime of $Cr(D_2O)_6^{3+}$ when diluted into different crystalline hosts reflects the sensitivity of the ^2E–$^4T_2$ gap to environment.

Endicott et al. have collected much of the extant information on Arrhenius parameters in Cr(III) complexes.[18] Some caution must be exercised in comparing these parameters since different solvent systems are involved and most of the fitting is to a one-term Arrhenius function. This problem is illustrated by $Cr(bpy)_3^{3+}$ in alcohol–water solvents (Figure 6). A single-term Arrhenius fit is inapplicable in this case,[91] but a two-term fit is quite satisfactory. More striking examples of the need for at least two terms are $Cr(NCS)_6^{3-}$ and *trans*-$Cr(NH_3)_2(NCS)_4^-$ in fluid acetone.[188] Endicott and co-workers have concluded, on the basis of the failure of the activation energy for a group of bis(polypyridine) complexes in DMSO/H_2O to correlate with the $^4T_2$–^2E gap, that solvent-assisted $^2E \rightarrow {}^4A_2$ is the dominant decay pathway.[97] While this conclusion may ultimately be validated, data from at least two of the complexes cannot be fitted to a one-term Arrhenius function. If these two complexes are omitted, the argument is less persuasive.

Endicott has employed an equation appropriate to the strong-coupling limit ($S \gg 1$) to fit the thermal decays in $Cr(NH_3)_6^{3+}$ and $Cr(cyclam)(CN)_2^+$.[175] He compared the activation energies obtained from this equation and by a conventional one-term Arrhenius fit. There was good concordance between the two values for $Cr(NH_3)_6^{3+}$ and $Cr(ND_3)_6^{3+}$, but not for $Cr(cyclam)(CN)_2^+$ and $Cr(D\text{-}cyclam)(CN)_2^+$.

When eq 17 is valid

$$\Phi_p/\tau = \eta_D k_5$$

Even though absolute quantum yields are difficult to obtain, the temperature dependence of relative Φ_p/τ can be used to infer changes in $\eta_D k_5$. The decay is mainly radiative and η_D is nearly unity when $Cr(CN)_6^{3-}$ is embedded in $K_3Co(CN)_6$.[173] The nearly twofold increase in Φ_p/τ in this crystalline system is attributable to thermal enhancement of k_5.[60] In an alcohol/H_2O solution, the $Cr(CN)_6^{3-}$ Φ_p/τ increases only slightly between 77 and 298 K.[154] A similar constancy obtains in an alcohol/H_2O solution of $Cr(en)_3^{3+}$. These results suggest that η_D is temperature independent in these systems.

Microenvironmental Heterogeneity. One of the most striking features of $^2E \rightarrow {}^4A_2$ emission is the very good exponentiality of the decay even in glassy solutions where environmental microheterogeneity prevails. This exponentiality is compromised when a proximate electronic state provides an alternative decay pathway, as exemplified by the $Cr(D_2O)_6^{3+}$ emission near 77 K.[138] If the nonexponentiality results from the variation in the small ^2E–$^4T_2$ gap with site in the rigid glass, back-transfer would be manifested by an increasing departure from exponentiality as the temperature is increased.[189] Since impurity emission also leads to nonexponentiality, it is necessary to establish that the decay becomes exponential at low temperatures before the decay profiles are used to infer back-transfer. This phenomenon is exhibited by the $Cr(NH_3)_{6-n}(H_2O)_n^{3+}$ complexes. In this series the $^4T_2$–^2E gap decreases progressively with n. The gap is large enough to inhibit $^2E \rightarrow {}^4T_2$ back-transfer when $n < 4$ and the microheterogeneity has no effect on the decay. In contrast, when $n > 3$, the gap becomes sufficiently small to permit some back-transfer, and nonexponentiality becomes detectable as the temperature is increased.[138]

The $Cr(ox)_3^{3-}$ decay in the $NaMgAl(ox)_3 \cdot 9H_2O$ host is exponential at all temperatures but is nonexponential at 77 K in DMSO/H_2O.[189] The nonexponentiality increases with temperature in the glass. Further evidence that the nonexponentiality in $Cr(ox)_3^{3-}$ is due to back-transfer comes from a comparison of the thermal decay behavior in the $Cr(en)_{3-n}(ox)_n^{3-2n}$ complexes, where the $^4T_2$–^2E gap decreases with n.[189] These data support Endicott's claim that the thermal decay in $Cr(en)_3^{3+}$ is not due to back-transfer.[187]

The thermally induced nonexponentiality in the ^2E decay of $Cr(acac)_3$ points to back-transfer as a relaxation pathway.[189]

Solvent Motions and Excited-State Decay. When the temperature range encompasses both glassy and fluid environments, the analysis can be more complicated. At one extreme stands *trans*-$Cr(cyclam)(NH_3)_2^{3+}$ in DMSO/H_2O, where the data can be reasonably well fitted to eq 14, providing that the small inflection near 150 K is ignored.[120] The ^2E decay is exponential from 77 to 325 K, and the Arrhenius parameters are $s_1 = 6 \times 10^3$ s^{-1}, $E_1 = 0.6$ kcal mol^{-1}, $s_2 = 1.3 \times 10^{15}$ s^{-1}, and

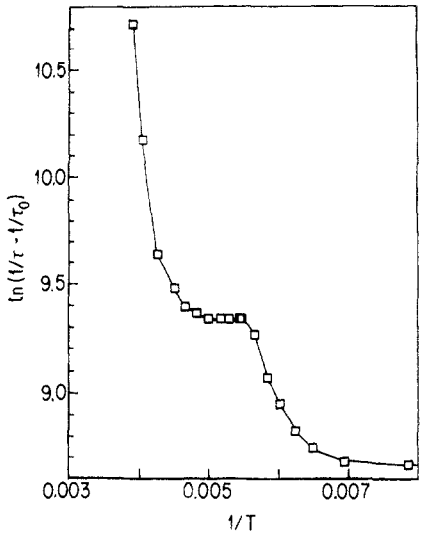

Figure 7. Temperature dependence of the *trans*-$Cr(py)_4F_2^+$ excited-state decay, corrected for the low-temperature limiting rate, in ethylene glycol/H_2O (2:1 (v/v)).

E_2 = 15.2 kcal mol^{-1}.[190] In contrast, the $^2E^Q$ decay of *trans*-$Cr(py)_4F_2^+$ in ethylene glycol–water is not represented by a multiterm Arrhenius expression (Figure 7). The sharp rate increase at 150 K is associated with solvent motions that reduces the $^2E^Q \rightarrow {}^4A_2$ transition energy.[91] This behavior is a clear indication of a transition region between two thexi states. Above 230 K the decay rate increase is well fitted by a single-term Arrhenius expression. When the solvent is changed to glycerol–water, which becomes fluid at a higher temperature, the plateau is reduced to an inflection. The viscosity does not follow an Arrhenius relation near the glass point, and these results indicate that considerable care must be exercised in the interpretation of thermal effects when abrupt viscosity changes are involved.

The thermal contribution to the decay in CrN_6^{3+} complexes is ligand sensitive, but in most cases the high-temperature process becomes important only after the solvent fluidity is high enough to allow for rapid solvent relaxation on the excited-state time scale. Examples are *trans*-$Cr(cyclam)(NH_3)_2^{3+}$ and $Cr(tacn)_2^{3+}$, where the photochemical yields are negligible.[184,191] E_2 is 6 kcal mol^{-1} larger in the former than in the latter complex. Although the $^4T_2$–^2E gap is smaller in $Cr(tacn)_2^{3+}$, the difference in this quantity is not sufficient to explain the change in the activation energy. Formation of a seven-coordinate intermediate with the solvent that decays nonradiatively to $^4A_2$ is a plausible thermal decay process.

While the dominant thermal decay pathway for CrN_6^{3+} complexes now seems to be established, it cannot be assumed that the same mechanism applies to CrN_4X_2 and CrN_5X complexes. Aside from the question of ^2E–$^2E^Q$ order, the uncertainty in the gap between the emitting level and the lowest energy quartet level requires that caution be exercised. The limited data now available suggest that back-transfer can be important in CrN_4X_2 and CrN_5X complexes when X is a weak-field ligand.[187,189]

D. Photochemistry and Photophysics

The photophysical observations consist of emission intensities excited by steady-state or pulsed sources and excited-state absorption following pulsed excitation. When emission and photoreaction can be measured under the same conditions, direct information about the reactive state can be obtained (for reviews, see refs 18 and 192–194). The observation of some photoreaction when ^2E emission is quenched is clear evidence for prompt $^4T_2$ photochemistry that precedes population of ^2E. One reaction where the entire photochemistry is unquenchable is $Cr(CN)_6^{3-}$ in DMF, proving that all of the photochemistry originates in $^4T_2$.[195] In contrast, nearly all of the $Cr(bpy)_3^{3-}$ reaction is quenchable.[196] The photoreaction is partially quenched in *trans*-$Cr(NH_3)_2(NCS)_4^-$, $Cr(en)_3^{3+}$, *trans*-$Cr(en)_2NH_3F^{2+}$,[193] and *trans*-$Cr(NH_3)_4CNX$ (X = NCS^-, CN^-, NH_3).[197] Even if all or part of the photoreaction is quenched when the doublet emission is reduced, ^2E is not necessarily the reactive level for the quenchable reaction, as attested by the longstanding controversy about the quenchable $Cr(en)_3^{3+}$ photochemistry. ^2E reaction cannot be distinguished from slow reaction in $^4T_2$ following back-transfer by the ^2E decay kinetics. Only if back-transfer can be ruled out, as in the case of CrN_6^{3+} complexes, can ^2E be identified as the reactive level by quenching measurements alone.

Although emission does provide data on excited-state chemistry that is absent in studies of ground-state kinetics, mechanistic details are still elusive. ^2E photochemistry has been characterized as direct or via a ground-state intermediate,[18] but identification of the reactive state does not distinguish a direct reaction in that state from one in which the state is merely a precursor to reaction. The direct ^2E reaction produces a primary product that is in an excited doublet state. The dissociative and associative limits of the direct primary process can be represented as

$$CrL_6^* \rightarrow CrL_5^* + L \quad (19a)$$

$$CrL_6^* + S \rightarrow CrL_6S^* \quad (19b)$$

The corresponding dissociative and associative limits of the ground-state intermediate mechanism are

$$CrL_6^* \rightarrow CrL_5 + L \quad (19c)$$

$$CrL_6^* + S \rightarrow CrL_6S \quad (19d)$$

Adamson has advanced empirical rules relating the ^2E lifetime to photochemistry for complexes in which back-transfer is negligible.[198] One of these rules suggests that a short ^2E lifetime at ambient temperatures is due to photolysis. Certainly, an increase in the rate of any of the processes in eq 19 will lead to a lifetime reduction. However, a decrease in the lifetime need not be due to an increased reaction rate. The lifetime of *trans*-$Cr(cyclam)(CN)_2^+$ is exceptionally high at ambient temperatures, and no reaction was detected.[140] The lack of thermal ^2E quenching was attributed to inhibition of reaction, while the very marked lifetime reduction at room temperature in *trans*-$Cr(en)_2(CN)_2^+$ was presumed to be the result of ^2E reaction.[140] The absence of photoreaction in *trans*-$Cr(cyclam)(NH_3)_2^{3+}$, coupled with a long room temperature lifetime,[184] would support the Adamson model. However, the room temperature lifetime of $Cr(sep)^{3+}$, where photolysis is inhibited by encapsulation, is nearly the same as that of $Cr(en)_3^{3+}$, where ^2E photoreaction is substantial.[199] Even more convincing evidence that photochemistry and photophysics need not be kinetically linked is the behavior

of $Cr(diamsar)^{3+}$, where the marked thermal ^2E decay is not accompanied by reaction.[131]

The absence of a kinetic contribution by reaction can be interpreted in terms of eq 19. If only emission from CrL_6* is monitored, the rate of direct dissociation (Eq 19a) could properly be described by k_{rx}, but the rate of eq 19c is more appropriately included in k_6. Both of the association reactions (eqs 19b and 19d) would lead to quenching of CrL_6*. However, neither of these reactions need lead to an overall photochemical change. Instead, the primary products could re-form CrL_6. In this event, eqs 19b and 19d would be described as solvent quenching.

In contrast to the usual situation in low-temperature glasses, the ^2E lifetime is often solvent dependent at ambient temperatures. Twofold lifetime variations are not uncommon.[191,198] The deuterium isotope effect nearly disappears at higher temperatures in CrN_6^{3+} complexes. On the basis of this result, the high-temperature process has been associated with a strong-coupling mechanism in which E_2 corresponds to the energy needed to reach the surface crossing between the excited and ground states.[184] The $Cr(bpy)_3^{3+}$ lifetime is especially sensitive to solvent and to counterion.[200] This latter complex is of especial interest since ^2E is the precursor to reaction. Although the emission lifetime is pH independent, the photolysis is suppressed by $[H^+]$. This can be rationalized by assuming that the primary photolytic product reacts in acid to re-form $Cr(bpy)_3^{3+}$, but it again illustrates the difficulty in correlating photophysical and photochemical results. Substituents on the ligands in $Cr(bpy)_3^{3+}$ have a much larger effect on the lifetime at ambient temperatures[201] than at low temperatures.[200] $k_{rx} \ll k_6$ in these complexes, and no connection between photochemistry and photophysics has been established. Except for the polypyridyl complexes, little data are available for solvent effects on both photochemistry and photophysics of a given complex.

A more direct way to detail the mechanism is to determine the dynamics of primary photoproduct formation. Several attempts to identify the primary product and the dynamics associated with its formation have been reported. The rise time for the formation of $Cr(en)_2(enH)H_2O^{4+}$ is the same as the luminescence decay time for $Cr(en)_3^{3+}$ emission.[203] This observation does not, in itself, distinguish an associative from a dissociative mechanism. At ambient temperatures solvent motions are fast on the ^2E lifetime scale and the dissociative mechanism would lead to a photoproduct rise time that is the same as the emission lifetime. The rise time for CrL_5S could also be identical with the ^2E lifetime in an associative process if eq 19b or 19d is rate limiting.

The ^2E emission lifetime of *cis*-$Cr(cyclam)(NH_3)_2^{3+}$ is 1.3 μs at ambient temperature. An intermediate, which was identified as *cis*-$Cr(cyclam)(H_2O)(NH_3)^{3+}$ and is formed more slowly than the ^2E state decay, has been detected by pulsed conductance measurements.[204] This result is consistent with an associative mechanism where the dissociation of CrL_6S is rate limiting but not with a dissociative mechanism.

V. Summary and Future Prospects

The lifetime results on Cr(III) complexes constitute the largest collection of photophysical data available for any single transition-metal ion. Most of the results refer to the $^2E \rightarrow {}^4A_2$ transition. When there are high-frequency ligand-localized accepting modes, e.g., N–H, the single-mode approximation in the weak-coupling limit provides a suitable framework for systematizing a broad range of data. In the absence of such high-frequency modes, ligand-induced changes in the electronic factor become more important, and no satisfactory model has yet been developed for relating these factors to molecular structure.

Although some understanding of the relationship between structure and the low-temperature k_6 has emerged, a comparable understanding of thermal influences on the nonradiative decay has developed more slowly. The nature of the process by which ^2E is thermally depopulated when back-transfer is inhibited by a large ^2E–$^4T_2$ gap has not yet been unambiguously identified. In particular, there are little data on the effect of solvent on the competition between photochemistry and photophysics in ^2E. Further work in this area may be expected.

The rarity of delayed fluorescence in complexes where back-transfer is expected is still poorly understood. Small changes in ligand structure affect k_3 more than k_6. Until complexes containing ligands with high-frequency accepting modes and with $^4T_2$ below ^2E can be synthesized, it will not be possible to make the same kind of study on k_3 that has been made for k_6.

Has the Cr(III) photophysical mine been played out? Should more effort be expended on one metal ion when the vast resources of other metals have scarcely been touched? History reveals that new technology can restore the viability of old mines. The dynamical study of primary photoprocesses as a function of solvent mobility from the subnanosecond to the millisecond time domains is one area that is ripe for exploitation. There is still some valuable Cr(III) ore left.

VI. Acknowledgments

I am grateful to all my studients and co-workers who are identified in the references. My especial thanks go to Dr. F. Castelli for many years of imaginative contributions and stimulating collaboration. Preparation of this review was supported by the donors of the Petroleum Research Fund, administered by the American Chemical Society. My research in this area has been supported by the National Science Foundation, the Petroleum Research Fund, and the Atomic Energy Commission.

VII. References

(1) Becquerel, E. *La lumiere, ses causes et ses effects*; Gauthier-Villars: Paris, 1867.
(2) Varsanyi, F.; Wood, D. L.; Schawlow, A. L. *Phys. Rev.* **1959**, *3*, 544.
(3) Finkelstein, R.; Van Vleck, J. H. *J. Chem. Phys.* **1940**, *8*, 790.
(4) DeArmond, K.; Forster, L. S. *J. Chem. Phys.* **1961**, *55*, 2193.
(5) DeArmond, K.; Forster, L. S. *Spectrochim. Acta* **1963**, *19*, 1403, 1687.
(6) Porter, G. B.; Schläfer, H. L. *Z. Phys. Chem. (Frankfurt)* **1963**, *38*, 227; **1964**, *40*, 280.
(7) Porter, G. B.; Schläfer, H. L. *Z. Phys. Chem. (Frankfurt)* **1963**, *37*, 109.
(8) Englman, R. *Non-Radiative Decay of Ions and Molecules*; North-Holland: Amsterdam, 1979.
(9) Freed, K. F. *Top. Appl. Phys.* **1976**, *15*, 1.
(10) Avouris, P.; Gelbart, W. M.; El-Sayed, M. A. *Chem. Rev.* **1977**, *77*, 793.

(11) Englman, R.; Jortner, J. *Mol. Phys.* **1970**, *18*, 145.
(12) Robbins, D. J.; Thomson, A. J. *Mol. Phys.* **1973**, *25*, 1103.
(13) Forster, L. S. *Transition Met. Chem.* **1969**, *5*, 1.
(14) Schläfer, H. L. *Z. Chem.* **1970**, *10*, 9.
(15) Kemp, T. J. *Prog. React. Kinet.* **1980**, *10*, 301.
(16) Forster, L. S. *Adv. Chem. Ser.* **1976**, *150*, 172.
(17) Fleischauer, P. D.; Fleischauer, P. *Chem. Rev.* **1970**, *70*, 199.
(18) Endicott, J. F.; Ramasami, T.; Tamilarasan, R.; Lessard, R. B.; Ryu, C. K.; Brubaker, G. R. *Coord. Chem. Rev.* **1987**, *77*, 1.
(19) Tanabe, Y.; Sugano, S. *J. Phys. Soc. Jpn.* **1954**, *9*, 753.
(20) Ohno, T.; Kato, S.; Kaizakl, S.; Hanazaki, I. *Inorg. Chem.* **1986**, *25*, 3853.
(21) Sugano, S.; Schawlow, A. L.; Varsanyi, F. *Phys. Rev.* **1960**, *120*, 2045.
(22) Güdel, H. U.; Snellgrove, T. R. *Inorg. Chem.* **1978**, *17*, 1617.
(23) Güdel, H. U. *Adv. Chem. Ser.* **1986**, *No. 307*, 1.
(24) Ferguson, J.; Wood, H. J.; Wood, D. L. *J. Chem. Phys.* **1971**, *54*, 504.
(25) Nelson, D. F.; Sturge, M. D. *Phys. Rev.* **1965**, *137*, A1117.
(26) Urushiyama, A.; Schönheer, T.; Schmidtke, H. H. *Ber. Bunsenges. Phys. Chem.* **1986**, *90*, 1188.
(27) Mortensen, O. S. *J. Chem. Phys.* **1967**, *47*, 4215.
(28) Geiser, U.; Güdel, H. U. *Inorg. Chem.* **1981**, *20*, 3013.
(29) Kaizaki, S.; Ito, M.; Nishimura, N.; Matsushita, Y. *Inorg. Chem.* **1985**, *24*, 2080.
(30) Hauser, A.; Mader, M.; Robinson, W. T.; Murugesan, R.; Ferguson, J. *Inorg. Chem.* **1987**, *26*, 1331.
(31) Courtois, M.; Forster, L. S. *J. Mol. Spectrosc.* **1965**, *18*, 396.
(32) Fields, R. A.; Winscom, C. J.; Haindl, E.; Plato, M.; Moebius, K. *Chem. Phys. Lett.* **1986**, *124*, 121.
(33) Schönherr, T.; Eyring, G.; Linder, R. *Z. Naturforsch.* **1983**, *38a*, 736.
(34) Fields, R. A.; Haindl, E.; Winscom, C. J.; Khan, Z. H.; Plato, M.; Moebius, K. *J. Chem. Phys.* **1984**, *80*, 3082.
(35) Flint, C. D.; Mathews, A. P. *J. Chem. Soc., Faraday Trans. 2* **1973**, *69*, 419.
(36) Shepard, W. N.; Forster, L. S. *Theor. Chim. Acta* **1971**, *20*, 135.
(37) DeCurtins, S.; Güdel, H. U.; Neuenschwander, K. *Inorg. Chem.* **1977**, *16*, 796.
(38) Le, K. Y.; Hoggard, P. E. *Inorg. Chem.* **1988**, *27*, 907.
(39) Schönherr, T.; Schmidtke, H. H. *Inorg. Chem.* **1979**, *18*, 2726.
(40) Riesen, H. *Inorg. Chem.* **1988**, *27*, 4677.
(41) Schmidtke, H. H.; Adamsky, H.; Schönherr, T. *Bull. Chem. Soc. Jpn.* **1988**, *61*, 59.
(42) Flint, C. D.; Mathews, A. P. *J. Chem. Soc., Faraday Trans. 2* **1980**, *76*, 1381.
(43) Flint, C. D.; Mathews, A. P. *Inorg. Chem.* **1975**, *14*, 1008.
(44) Perumareddi, J. R. *J. Phys. Chem.* **1967**, *71*, 3444, 3455.
(45) Perumareddi, J. R. *Coord. Chem. Rev.* **1969**, *4*, 73.
(46) Glerup, J.; Mønsted, O.; Schäffer, C. E. *Inorg. Chem.* **1976**, *15*, 1399.
(47) Hoggard, P. E. *Z. Naturforsch.* **1981**, *36a*, 1276.
(48) Lever, A. P. B. *Inorganic Electronic Spectroscopy*, 2nd ed.; Elsevier: Amsterdam, 1984.
(49) Hoggard, P. E. *Coord. Chem. Rev.* **1986**, *70*, 85.
(50) Demas, J. N.; Crosby, G. A. *J. Am. Chem. Soc.* **1970**, *92*, 7762.
(51) Rojas, G.; Magde, D. *Chem. Phys. Lett.* **1983**, *102*, 399.
(52) Klassen, D. M.; Schläfer, H. L. *Ber. Bunsenges. Phys. Chem.* **1968**, *72*, 663.
(53) Köglin, E.; Krasser, W. *Z. Naturforsch.* **1973**, *28a*, 1131.
(54) Schläfer, H. L.; Gausmann, H.; Zander, H. U. *Inorg. Chem.* **1967**, *6*, 1528.
(55) Fleischauer, P. D.; Adamson, A. W.; Sartori, G. *Prog. Inorg. Chem.* **1972**, *17*, 1.
(56) Targos, W.; Forster, L. S. *J. Chem. Phys.* **1966**, *44*, 4342.
(57) Condrate, R. A.; Forster, L. S. *J. Mol. Spectrosc.* **1967**, *24*, 490.
(58) Castelli, F.; Forster, L. S. *J. Am. Chem. Soc.* **1975**, *97*, 6306.
(59) Watson, W. M.; Wang, Y.; Yardley, J. T.; Stucky, G. D. *Inorg. Chem.* **1975**, *14*, 2374.
(60) Camassei, F. D.; Forster, L. S. *J. Chem. Phys.* **1969**, *50*, 2603.
(61) Otto, H.; Yersin, H.; Gliemann, G. *Z. Phys. Chem. (Frankfurt)* **1974**, *92*, 193.
(62) König, E. J.; Lindner, E.; Lorenz, I. P.; Gitter, G. *Inorg. Nucl. Chem.* **1971**, *33*, 3305.
(63) Kisliuk, P.; Moore, C. A. *Phys. Rev.* **1967**, *160*, 307.
(64) Walling, J. C.; Jenssen, H. P.; Morris, R. C.; O'Dell, E. W.; Peterson, O. G. *Opt. Lett.* **1979**, *4*, 182.
(65) Henry, M. O.; Larkin, J. P.; Imbusch, G. F. *Phys. Rev.* **1976**, *B13*, 1893.
(66) Castelli, F.; Forster, L. S. *Phys. Rev.* **1975**, *B11*, 920.
(67) Reisfeld, R.; Jørgensen, C. K. *Struct. Bonding* **1988**, *69*, 63.
(68) Andrews, L. J.; Lempicki, A.; McCollum, B. C. *J. Chem. Phys.* **1981**, *74*, 5526.
(69) Köglin, E.; Krause, W. *Ber. Bunsenges. Phys. Chem.* **1972**, *76*, 401.
(70) Cancellieri, P.; Cervone, E.; Furlani, C.; Sartori, G. *Z. Phys. Chem. (Frankfurt)* **1968**, *62*, 35.
(71) DeArmond, K.; Mitchell, W. J. *Inorg. Chem.* **1972**, *11*, 18.
(72) Angel, S. M.; DeArmond, M. K. *Inorg. Chim. Acta* **1985**, *97*, 53.
(73) Ballhausen, C. J.; Bak, T. A. *J. Mol. Struct.* **1980**, *59*, 265.
(74) Flint, C. D.; Mathews, A. P. *J. Chem. Soc., Faraday Trans. 2* **1974**, *70*, 1301.
(75) Flint, C. D.; Greenough, P. *J. Chem. Soc., Faraday Trans. 2* **1974**, *70*, 815.
(76) Flint, C. D.; Mathews, A. P. *J. Chem. Soc., Faraday Trans. 2* **1976**, *72*, 579.
(77) Flint, C. D.; Palacio, D. J. D. *J. Chem. Soc., Faraday Trans. 2* **1980**, *76*, 82.
(78) Flint, C. D.; Greenough, P.; Mathews, A. P. *J. Chem. Soc., Faraday Trans. 2* **1973**, *69*, 23.
(79) Flint, C. D.; Palacio, D. J. D. *J. Chem. Soc., Faraday Trans. 2* **1977**, *73*, 649.
(80) Flint, C. D. *J. Chem. Soc., Faraday Trans. 2* **1976**, *72*, 721.
(81) Flint, C. D. *Coord. Chem. Rev.* **1974**, *14*, 47.
(82) Forster, L. S.; Rund, J. V.; Fucaloro, A. F. *J. Phys. Chem.* **1984**, 88, 5012.
(83) Flint, C. D.; Greenough, P. *J. Chem. Soc., Faraday Trans. 2* **1972**, *68*, 897.
(84) Forster, L. S.; Mønsted, O. *J. Phys. Chem.* **1986**, *90*, 513.
(85) Flint, C. D.; Mathews, A. P. *J. Chem. Soc., Faraday Trans. 2* **1974**, *70*, 1307.
(86) Ghaith, A. M.; Forster, L. S.; Rund, J. V. *Inorg. Chem.* **1987**, *26*, 2493.
(87) Fucaloro, A. F.; Forster, L. S.; Glover, S. G.; Kirk, A. D. *Inorg. Chem.* **1985**, *24*, 4242.
(88) Dubicki, L.; Hitchman, M. A.; Day, P. *Inorg. Chem.* **1970**, *9*, 188.
(89) Kirk, A. D.; Porter, G. B. *J. Phys. Chem.* **1980**, *84*, 887.
(90) Glover, S. G.; Kirk, A. D. *Inorg. Chim. Acta* **1982**, *64*, L139.
(91) Ghaith, A.; Forster, L. S.; Rund, J. V. *J. Phys. Chem.* **1988**, *92*, 6197.
(92) Ceulemans, A.; Beyens, D.; Vanquickenbourne, L. G. *J. Am. Chem. Soc.* **1982**, *104*, 2988.
(93) Ceulemans, A.; Bongaerts, N.; Vanquickenbourne, L. G. *Inorg. Chem.* **1987**, *26*, 1566.
(94) König, E.; Kremer, S. *Ligand Field Energy Diagrams*; Plenum: New York, 1977.
(95) Smith, D. W. *Inorg. Chem.* **1978**, *17*, 3153.
(96) Gerlach, M.; Wooley, R. G. *Prog. Inorg. Chem.* **1984**, *31*, 371.
(97) Ryu, C. K.; Endicott, J. K. *Inorg. Chem.* **1988**, *27*, 2203.
(98) Yuen, G.; Heaster, H.; Hoggard, P. E. *Inorg. Chim. Acta* **1981**, *73*, 231.
(99) Flint, C. D.; Mathews, A. P. *J. Chem. Soc., Faraday Trans. 2* **1975**, *71*, 379.
(100) Forster, L. S., unpublished.
(101) Camassei, F. D.; Forster, L. S. *J. Mol. Spectrosc.* **1969**, *31*, 129.
(102) Armendarez, P. X.; Forster, L. S. *J. Chem. Phys.* **1964**, *40*, 273.
(103) Köglin, E.; Krasser, W.; Wolff, G.; Nurnberg, H. W. *Z. Naturforsch.* **1974**, *29a*, 211.
(104) Coleman, W. F.; Forster, L. S. *J. Lumin.* **1971**, *4*, 429.
(105) Coleman, W. F. *J. Lumin.* **1980**, *22*, 17.
(106) Coleman, W. F. *J. Lumin.* **1975**, *10*, 163.
(107) Kawasaki, Y.; Forster, L. S. *J. Chem. Phys.* **1969**, *50*, 1010.
(108) Adamson, A. W. *J. Chem. Educ.* **1983**, *60*, 797.
(109) Schläfer, H. L.; Martin, M.; Gausmann, H.; Schmidtke, H. H. *Z. Phys. Chem.* **1971**, *76*, 61.
(110) Tuszynski, W.; Strauss, E. *J. Lumin.* **1988**, *40–41*, 276.
(111) Krause, R. *J. Phys. Chem.* **1978**, *82*, 2579.
(112) Harriman, A. *J. Chem. Soc., Faraday Trans. 1* **1982**, *78*, 2727.
(113) Gouterman, M.; Hanson, L. K.; Khalil, G. E.; Leenstra, W. R.; Buchler, J. W. *J. Chem. Phys.* **1975**, *62*, 2343.
(114) Ditze, A.; Wasgestian, F. *Ber. Bunsenges. Phys. Chem.* **1986**, *90*, 111.
(115) Zander, H.-U. Doctoral Dissertation, Johann Wolfgang Goethe University, Frankfurt A/M, 1969.
(116) Chatterjee, K. K.; Forster, L. S. *Spectrochim. Acta* **1964**, *20*, 1603.
(117) Demas, J. N.; Crosby, G. A. *J. Phys. Chem.* **1971**, *75*, 991.
(118) Carlin, R. L.; Walker, I. M. *J. Chem. Phys.* **1966**, *46*, 3921.
(119) Castelli, F.; Forster, L. S. *J. Lumin.* **1974**, *8*, 252.
(120) Fucaloro, A. F.; Forster, L. S. *Inorg. Chim. Acta* **1987**, *132*, 253.
(121) Siebrand, W. In *Dynamics of Molecular Collisions*; Miller, W. H., Ed.; Plenum: New York, 1976; Part A, Chapter 6.
(122) Schuurmans, M. F. H.; van Dijk, J. M. F. *Physica* **1984**, *123B*, 131.
(123) Siebrand, W.; Zgierski, M. Z. *Chem. Phys. Lett.* **1975**, *35*, 151. (a) Lin, S. H.; Bersohn, R. *J. Chem. Phys.* **1968**, *48*, 2732.
(124) Siebrand, W. In *The Triplet State*; Zahlan, A. B., Ed.; Cambridge University Press: London, 1967; p 31.
(125) Van Dijk, J. M. F.; Schuurmans, M. F. H. *J. Chem. Phys.* **1983**, *78*, 5317.
(126) Strek, W.; Ballhausen, C. *J. Mol. Phys.* **1978**, *36*, 1321.
(127) Strek, W. *Acta Phys. Polon.* **1980**, *A60*, 707.

(128) Kupka, H. *Mol. Phys.* **1979**, *37*, 1673.
(129) Kühn, K.; Wasgestian, F.; Kupka, H. *J. Phys. Chem.* **1981**, *85*, 665.
(130) Comba, P.; Creaser, I. I.; Gahan, L. R.; Harrowfield, J. M.; Lawrance, G. A.; Martin, L. L.; Mau, A. W. H.; Sargeson, A. M.; Sasse, W. H. F.; Snow, M. *Inorg. Chem.* **1986**, *25*, 384.
(131) Comba, P.; Mau, A. W. H.; Sargeson, A. M. *J. Phys. Chem.* **1985**, *89*, 394.
(132) Ryu, C. K.; Lessard, R. B.; Lynch, D.; Endicott, J. F. *J. Phys. Chem.* **1989**, *93*, 1752.
(133) Weighhardt, K.; Tolksdorf, I.; Herrmann, W. *Inorg. Chem.* **1985**, *24*, 1230.
(134) Goldsmith, G. J.; Shallcross, F. V.; McClure, D. S. *J. Mol. Spectrosc.* **1965**, *16*, 296.
(135) Forster, L. S. In *Excited States of Transition Elements*; Jezowska-Trzbiatowska, B., Legrendziewicz, J., Strek, W., Eds.; World Scientific: Singapore, 1989; p 127.
(136) Mvele, M.; Wasgestian, F. *Spectrochim. Acta* **1986**, *42A*, 775.
(137) Mvele, M.; Wasgestian, F. *Inorg. Chim. Acta* **1986**, *119*, 25.
(138) Fucaloro, A. F.; Forster, L. S.; Rund, J. V.; Lin, S. H. *J. Phys. Chem.* **1983**, *87*, 1796.
(139) Wasgestian, F., private communication.
(140) Kane-Maguire, N. A. P.; Crippen, W. S.; Miller, P. K. *Inorg. Chem.* **1983**, *22*, 696.
(141) Castelli, F.; Forster, L. S. *J. Am. Chem. Soc.* **1973**, *95*, 7223.
(142) Conti, C.; Forster, L. S. *J. Am. Chem. Soc.* **1977**, *99*, 613.
(143) Buckels, H. W.; Wasgestian, F. *Ber. Bunsenges. Phys. Chem.* **1983**, *87*, 154.
(144) Chatterjee, K. K.; Porter, G. B. *Inorg. Chem.* **1966**, *5*, 860.
(145) Bartram, R. H. *Springer Ser. Opt. Sci.* **1985**, *47*, 155.
(146) Strek, W.; Lukowiak, E.; Hanuga, J.; Mugenski, E.; Cywinski, R. *J. Mol. Struct.* **1984**, *115*, 497.
(147) Kenyon, P. T.; Andrews, L. J.; McCollum, B.; Lempicki, A. *IEEE J. Quantum Electron.* **1982**, *QE-18*, 1189.
(148) Dürr, U.; Brauch, U.; Knierim, W.; Schiller, C. In *Tunable Solid State Lasers*; Springer-Verlag: Berlin, 1985; Vol. 47, p 20.
(149) Andrews, L. J.; Lempicki, A.; McCollum, B. C. *Chem. Phys. Lett.* **1980**, *74*, 404.
(150) Hush, N. S.; Hobbs, R. J. M. *Prog. Inorg. Chem.* **1969**, *10*, 259.
(151) Glass, A. M. *J. Chem. Phys.* **1969**, *50*, 1501.
(152) Serpone, N.; Hoffman, M. Z. *J. Phys. Chem.* **1987**, *91*, 1737.
(153) Rojas, G.; Magde, D. *Inorg. Chem.* **1987**, *26*, 2334.
(154) Castelli, F.; Forster, L. S. *J. Phys. Chem.* **1977**, *81*, 403.
(155) Pyke, S. C.; Windsor, M. W. *J. Am. Chem. Soc.* **1978**, *100*, 6518.
(156) LeSage, R.; Sala, K. L.; Yip, R. W.; Langford, C. H. *Can. J. Chem.* **1983**, *61*, 2761.
(157) Rojas, G. E.; Dupuy, C.; Sexton, D. A.; Magde, D. *J. Phys. Chem.* **1986**, *90*, 87.
(158) Serpone, N.; Jamieson, M. A.; Sharma, P. K.; Danesh, R.; Bolletta, F.; Hoffman, M. Z. *Chem. Phys. Lett.* **1984**, *104*, 87.
(159) Rojas, G.; Magde, D. *J. Phys. Chem.* **1987**, *91*, 689.
(160) Kirk, A. D.; Porter, G. B.; Sharma, D. K. *Chem. Phys. Lett.* **1986**, *123*, 548.
(161) Serpone, N.; Jamieson, M. A. *Coord. Chem. Rev.* **1989**, *93*, 87.
(162) Kirk, A. D.; Rampi Scandola, M. A. *J. Phys. Chem.* **1982**, *86*, 414.
(163) Ballardini, R.; Varani, G.; Wasgestian, H. F.; Moggi, L.; Balzani, V. *J. Phys. Chem.* **1973**, *77*, 2947.
(164) Yang, X.; Sutton, C. A.; Kutal, C. *Inorg. Chem.* **1982**, *21*, 2893.
(165) Kane-Maguire, N. A. P.; Phifer, J. E.; Toney, C. G. *Inorg. Chem.* **1976**, *15*, 593.
(166) Kane-Maguire, N. A. P.; Richardson, D. E.; Toney, C. G. *J. Am. Chem. Soc.* **1976**, *98*, 3996.
(167) Kane-Maguire, N. A. P.; Helwic, N.; Derrick, J. N. *Inorg. Chim. Acta* **1985**, *102*, L21.
(168) Conti, C.; Castelli, F.; Forster, L. S. *Inorg. Chim. Acta* **1979**, *33*, L171.
(169) Kirk, A. D.; Namasivayam, C. *Inorg. Chem.* **1983**, *22*, 2961.
(170) Sandrini, D.; Gandolfi, M. T.; Moggi, L.; Balzani, V. *J. Am. Chem. Soc.* **1978**, *100*, 1463.
(171) Sabbatini, N.; Scandola, M. A.; Balzani, V. *J. Phys. Chem.* **1974**, *78*, 541.
(172) Binet, D. J.; Goldberg, E. L.; Forster, L. S. *J. Phys. Chem.* **1968**, *72*, 3017.
(173) Castelli, F.; Forster, L. S. *J. Phys. Chem.* **1974**, *78*, 2122.
(174) Castelli, F.; Forster, L. S. *Chem. Phys. Lett.* **1975**, *30*, 465.
(175) Endicott, J. F.; Tamilarasan, R.; Lessard, R. B. *Chem. Phys. Lett.* **1984**, *112*, 381.
(176) Schläfer, H. L.; Gausmann, H.; Witzke, H. *Z. Phys. Chem. (Frankfurt)* **1967**, *56*, 55; *J. Chem. Phys.* **1967**, *46*, 1423.
(177) Pfeil, A. *J. Am. Chem. Soc.* **1971**, *93*, 5395.
(178) Gutierrez, A.; Adamson, A. W. *J. Phys. Chem.* **1978**, *82*, 902.
(179) Shipley, N. J.; Linck, R. G. *J. Phys. Chem.* **1980**, *84*, 2490.
(180) Adamson, A. W.; Gutierrez, A. R. *J. Phys. Chem.* **1980**, *84*, 2492.
(181) Forster, L. S.; Castelli, F. *J. Phys. Chem.* **1980**, *84*, 2492.
(182) Linck, N. J.; Behrens, S. J.; Magde, D.; Linck, R. G. *J. Phys. Chem.* **1983**, *87*, 1733.
(183) Kane-Maguire, N. A. P.; Clounts, G. M.; Kerr, R. C. *Inorg. Chim. Acta* **1980**, *44*, L157.
(184) Kane-Maguire, N. A. P.; Wallace, K. C.; Miller, D. B. *Inorg. Chem.* **1985**, *24*, 597.
(185) Lin, S. H. *J. Chem. Phys.* **1972**, *56*, 2648.
(186) Allsopp, S. R.; Cox, A.; Kemp, T. J.; Reed, W. J.; Sostero, S.; Traverso, O. *J. Chem. Soc., Faraday Trans. 1* **1980**, *76*, 162.
(187) Lessard, R. B.; Endicott, J. F.; Perkovic, M. W.; Ochrymowiycz, L. A. *Inorg. Chem.* **1989**, *28*, 2574.
(188) Kang, Y.; Castelli, F.; Forster, L. S. *J. Phys. Chem.* **1979**, *83*, 2368.
(189) Forster, L. S.; Murrow, D.; Fucaloro, A. F. *Inorg. Chem.*, submitted.
(190) Murrow, D.; Forster, L. S., unpublished.
(191) Ditze, A.; Wasgestian, F. *J. Phys. Chem.* **1985**, *89*, 426.
(192) Kirk, A. D. *Coord. Chem. Rev.* **1981**, *39*, 225.
(193) Kirk, A. D. *J. Chem. Educ.* **1983**, *60*, 843.
(194) Adamson, A. W. *Comments Inorg. Chem.* **1981**, *1*, 33.
(195) Wasgestian, H. F. *J. Phys. Chem.* **1972**, *76*, 1947.
(196) Maestri, M.; Bolletta, F.; Moggi, L.; Balzani, V.; Henry, M. S.; Hoffman, M. Z. *J. Am. Chem. Soc.* **1978**, *100*, 2694.
(197) Riccieri, P.; Zinato, E.; Diamiani, A. *Inorg. Chem.* **1987**, *26*, 2667.
(198) Walters, R. T.; Adamson, A. W. *Acta Chem. Scand.* **1979**, *A33*, 53.
(199) Ramasami, T.; Endicott, J. F.; Brubaker, G. R. *J. Phys. Chem.* **1983**, *87*, 5057.
(200) Henry, M. S.; Hoffman, M. Z. *Adv. Chem. Ser.* **1978**, *No. 168*, 91.
(201) Jamieson, M. A.; Serpone, N.; Hoffman, M. Z. *Coord. Chem. Rev.* **1981**, *39*, 121.
(202) Ghaith, A. Ph.D. Dissertation, University of Arizona, 1987.
(203) Fukuda, R.; Walters, R. T.; Macke, H.; Adamson, A. W. *J. Phys. Chem.* **1979**, *83*, 2097.
(204) Waltz, W. L.; Lee, S. H.; Friesen, D. A.; Lillie, S. *Inorg. Chem.* **1988**, *27*, 1132.
(205) Forster, L. S.; Rund, J. V.; Fucaloro, A. F.; Lin, S. H. *J. Phys. Chem.* **1984**, *88*, 5017.
(206) Endicott, J. F.; Lessard, R. B.; Lei, Y.; Ryu, C. K.; Tamilarasan, R. *ACS Symp. Ser.* **1986**, *307*, 85.
(207) Fucaloro, A. F.; Forster, L. S., unpublished.
(208) Kane-Maguire, N. A. P.; Wallace, K. C.; Cobranchi, D. P.; Derrick, J. M.; Speece, D. G. *Inorg. Chem.* **1986**, *25*, 2101.
(209) Strek, W.; Lukowiak, E.; Jezowska-Trzebiatowska, B. S. *J. Lumin.* **1977**, *15*, 437.
(210) Mitchell, W. S.; DeArmond, M. K. *J. Lumin.* **1971**, *4*, 137.
(211) Serpone, N.; Jamieson, M. A.; Henry, M. S.; Hoffman, M. Z.; Bolletta, F.; Maestri, M. *J. Am. Chem. Soc.* **1979**, *101*, 2907.
(212) Forster, L. S.; Rund, J. V.; Castelli, F.; Adams, P. *J. Phys. Chem.* **1982**, *86*, 2395.
(213) Kane-Maguire, N. A. P.; Wallace, K. C.; Speece, D. G. *Inorg. Chem.* **1986**, *25*, 4650.
(214) Candori, R.; Masetti, F.; Zinato, E. *Gazz. Chim. Ital.* **1973**, *103*, 885.
(215) Ghaith, A.; Forster, L. S.; Rund, J. V. *Inorg. Chim. Acta* **1986**, *16*, 11.
(216) McFarlane, R. M. *Phys. Rev.* **1970**, *B1*, 989.
(217) Wood, D. L.; Imbusch, G. F.; McFarlane, R. M.; Kisliuk, P.; Larkin, D. M. *J. Chem. Phys.* **1968**, *48*, 5255.